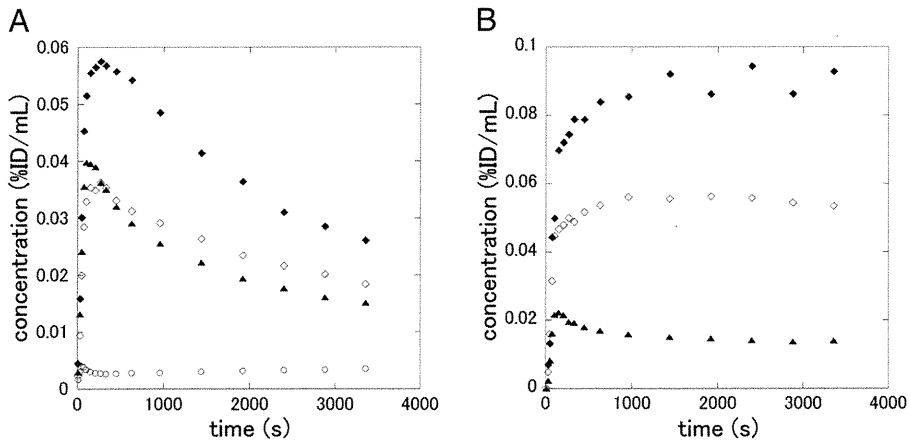

Fig. 4. The TACs for [^{18}F]FEP-4MA (A) and [^{11}C]MP4A (B) in the occipital cortex (closed triangle), cerebellum (open diamond) and striatum (closed diamond) of the monkey. The open circles in panel A indicate the TAC of the alcoholic metabolite of [^{18}F]FEP-4MA in the brain, which was infused via the crural vein in the same manner as in the [^{18}F]FEP-4MA experiment. All data represent decay corrected measured values.

the tracer β-value was over 0.1, k_3 precision was drastically decreased. The boundary value was not dependent on the k_2- and k_3-value of a tracer (data not shown). The decrease of k_3 precision with the increase of the tracer k_{el}-value may be attributed not only to the decrease of the total counts of radioactivity due to the reduction of the retention of the tracer, but also to the decrease of TAC sensitivity due to the tracer β-value being over 0.1. On the other hand, the extent of change in TAC shape with k_3 change was increased when the β-value was close to 0, suggesting that the β-value of a given tracer is preferred as low as possible for static analysis. These results indicate that, in addition to the α-value, the β-value is an important factor in determining tracer sensitivity.

To validate our simulation results, dynamic PET scans were performed in a monkey using two model tracers, [^{18}F]FEP-4MA and [^{11}C]MP4A. The biochemical and kinetic properties of both tracers have been well characterized. The finding that the uptake of [^{18}F]FEP-4MA into a brain was higher than that of [^{11}C]MP4A may reflect the higher lipophilicity of [^{18}F]FEP-4MA (Kikuchi et al., 2005). The α-value of [^{18}F]FEP-4MA was within the optimal α-value range ($\alpha = 0.70$). In [^{18}F]FEP-4MA, the values of the parameter reflecting the elimination of tracer metabolite were relatively low; (β, k_{el}) = (0.085, 0.012). These properties of [^{18}F]FEP-4MA resulted in high k_3 precision (SE = 7.4%). The high uptake of [^{18}F]FEP-4MA and slow decay of ^{18}F compared with ^{11}C may also be contributed to the high precision (Supplementary Fig. B). The precision of k_3 estimation was also high in [^{11}C]MP4A (SE = 10%) with (α, β) = (0.79, 0.028). These results indicate that the availability of a tracer with metabolite elimination should be determined by both the α- and β-values. On the basis of these results, we propose that the β-value, rather than k_{el}-value, is a fundamental kinetic parameter for determining the precision of k_3 estimation.

Conclusions

Our results revealed that the precision of k_3 estimation for a tracer is determined by both its α- and β-value; within the optimal α range of approximately 0.2–1, and with optimal values of $\beta < 0.1$. The incompleteness of the trapping of a tracer metabolite lowers the tracer sensitivity to changes in k_3. However, when the elimination rate is relatively low compared with the k_2-value (i.e. k_{el}-values satisfying the optimal β condition) a tracer is expected to show high sensitivity.

Acknowledgments

We thank the technical team of the Cyclotron Section and Radiopharmaceuticals Section of the National Institute of Radiological Sciences for their support during cyclotron operation and the production of radioisotopes.

Appendix A. Supplementary data

Supplementary data to this article can be found online at doi:10.1016/j.neuroimage.2011.02.030.

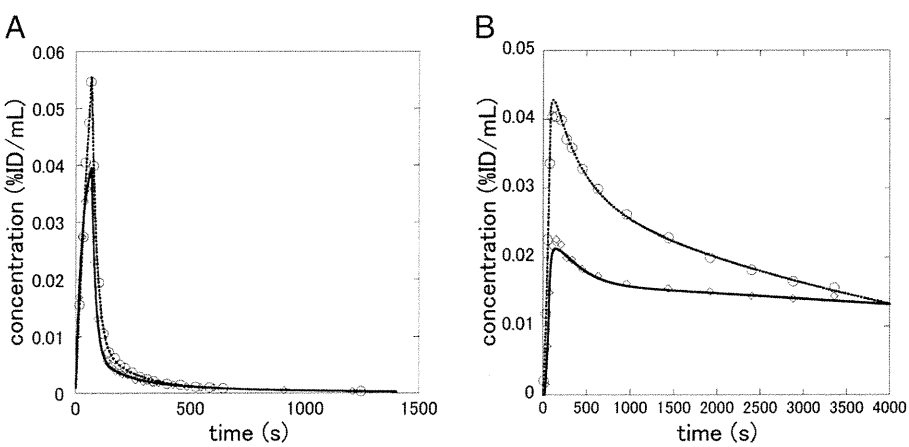

Fig. 5. The TACs of authentic [^{18}F]FEP-4MA and [^{11}C]MP4A in arterial plasma (A), and the TACs for the both tracers in occipital cortex (B) in a monkey. Open circles and open diamonds indicate the decay corrected measured values for [^{18}F]FEP-4MA and [^{11}C]MP4A, and the dotted and solid lines show fitted curves for both, respectively.

Table 1
Rate constants of occipital cortex in monkey.

	Rate constants (mean ± SD)				α-value
	K_1	k_2	k_3	k_{el}	
	$mLg^{-1}min^{-1}$	min^{-1}			
[^{18}F]FEP-4MA	0.65 ± 0.055	0.14 ± 0.026	0.10 ± 0.017 (SE 7.4%)	0.012 ± 0.0010	0.70
[^{11}C]MP4A	0.47 ± 0.023†	0.13 ± 0.012	0.10 ± 0.014 (SE 10%)	0.0036 ± 0.0013†	0.79

Table shows averaged values of six ROIs in occipital cortex of a single monkey. Standard errors (SE) of k_3 estimates calculated from the mean TAC of six ROIs are presented in parentheses. $^{\dagger}P<0.01$ for each rate parameter for [^{18}F]FEP-4MA vs. that for [^{11}C]MP4A in unpaired, two-tailed Student's *t*-tests.

References

Carson, R.E., 1986. Parameter estimation in positron emission tomography. In: Phelps, M., Mazziotta, J., Schelbert, H. (Eds.), Positron Emission Tomography and Autoradiography. Raven Press, New York, pp. 347–390.

Friberg, L., Andersen, A.R., Lassen, N.A., Holm, S., Dam, M., 1994. Retention of ^{99m}Tc-Bicisate in the human brain after intracarotid injection. J. Cereb. Blood Flow Metab. 14 (Suppl. 1), S19–S27.

Fukushi, K., Iyo, M., Irie, T., Namba, H., 1993. In vivo mapping of acetylcholinesterase (AChE) in the brain by radioactive acetylcholine analogues: Sensitivity analysis of non-linear tracer response for PET application. J. Cereb. Blood Flow Metab. Suppl. 1, S279.

Iida, H., Higano, S., Tomura, N., Shishido, F., Kanno, I., Miura, S., Murakami, M., Takahashi, K., Sasaki, H., Uemura, K., 1988. Evaluation of regional differences of tracer appearance time in cerebral tissues using [^{15}O]water and dynamic positron emission tomography. J. Cereb. Blood Flow Metab. 8, 285–288.

Iyo, M., Namba, H., Fukushi, K., Shinotoh, H., Nagatsuka, S., Suhara, T., Sudo, Y., Suzuki, K., Irie, T., 1997. Measurement of acetylcholinesterase by positron emission tomography in the brains of healthy controls and patients with Alzheimer's disease. Lancet 349, 1805–1809.

Kikuchi, T., Zhang, M.R., Ikota, N., Fukushi, K., Okamura, T., Suzuki, K., Arano, Y., Irie, T., 2005. N-[^{18}F]fluoroethylpiperidin-4ylmethyl acetate, a novel lipophilic acetylcholine analogue for PET measurement of brain acetylcholinesterase activity. J. Med. Chem. 48, 2577–2583.

Kikuchi, T., Okamura, T., Zhang, M.R., Fukushi, K., Irie, T., 2010. In vivo evaluation of N-[^{18}F]fluoroethylpiperidin-4ylmethyl acetate in rats compared with MP4A as a probe for measuring cerebral acetylcholinesterase activity. Synapse 64, 209–215.

Koeppe, R.A., Frey, K.A., Mulholland, F.G., Kilbourn, M.R., Buck, A., Lee, K.S., Kuhl, D.E., 1994. [^{11}C]Tropanyl benzilate-binding to muscarinic cholinergic receptors: methodology and kinetic modeling alternatives. J. Cereb. Blood Flow Metab. 14, 85–99.

Koeppe, R.A., Frey, K.A., Snyder, S.E., Meyer, P., Kilbourn, M.R., Kuhl, D.E., 1999. Kinetic modeling of N-[^{11}C] Methylpiperidine-4-yl propionate: alternatives for analysis of an irreversible positron emission tomography tracer for measurement of acetylcholinesterase activity in human brain. J. Cereb. Blood Flow Metab. 19, 1150–1163.

Lassen, N.A., Andersen, A.R., Friberg, L., Paulson, O.B., 1988. The retention of [99mTc]-d, l-HM-PAO in the human brain after intracarotid bolus injection: a kinetic analysis. J. Cereb. Blood Flow Metab. 8, S13–S22.

Levenberg, K., 1944. A method for the solution of certain non-linear problems in least squares. Q. Appl. Math. 2, 164–168.

Logan, J., Fowler, J.S., Volkow, N.D., Ding, Y.S., Wang, G.J., Alexoff, D.L., 2001. A strategy for removing the bias in the graphical analysis method. J. Cereb. Blood Flow Metab. 21, 307–320.

Logan, J., Fowler, J.S., Ding, Y.S., Franceschi, D., Wang, G.J., Volkow, N.D., Felder, C., Alexoff, D., 2002. Strategy for the formation of parametric images under conditions of low injected radioactivity applied to PET studies with the irreversible monoamine oxidase A tracers [^{11}C]clorgyline and deuterium-substituted [^{11}C] clorgyline. J. Cereb. Blood Flow Metab. 22, 1367–1376.

Marquardt, D.W., 1963. An algorithm for least-squares estimation of nonlinear parameters. J. Soc. Indust. Appl. Math. 11, 431–441.

Nagatsuka, S., Fukushi, K., Shinotoh, H., Namba, H., Iyo, M., Tanaka, N., Aotsuka, A., Ota, T., Tanada, S., Irie, T., 2001. Kinetic analysis of [^{11}C]MP4A using a high-radioactivity brain region that represents an integrated input function for measurement of cerebral acetylcholinesterase activity without arterial blood sampling. J. Cereb. Blood Flow Metab. 21, 1354–1366.

Namba, H., Iyo, M., Fukushi, K., Shinotoh, H., Nagatsuka, S., Suhara, T., Sudo, Y., Suzuki, K., Irie, T., 1999. Human cerebral acetylcholinesterase activity measured with positron emission tomography: procedure, normal values and effect of age. Eur. J. Nucl. Med. 26, 135–143.

Okamura, T., Kikuchi, T., Fukushi, K., Arano, Y., Irie, T., 2007. A novel noninvasive method for assessing glutathione-conjugate efflux systems in the brain. Bioorg. Med. Chem. 15, 3127–3133.

Okamura, T., Kikuchi, T., Okada, M., Toramatsu, C., Fukushi, K., Takei, M., Irie, T., 2009. Noninvasive and quantitative assessment of the function of multidrug resistance-associated protein 1 in the living brain. J. Cereb. Blood Flow Metab. 29, 504–511.

Shinotoh, H., Fukushi, K., Nagatsuka, S., Irie, T., 2004. Acetylcholinesterase imaging: its use in therapy evaluation and drug design. Curr. Pharm. Des. 10, 1505–1517.

Tsukada, H., Nishiyama, S., Kakiuchi, T., Ohba, H., Sato, K., Harada, N., Nakanishi, S., 1999. Isoflurane anesthesia enhances the inhibitory effects of cocaine and GBR12909 on dopamine transporter: PET studies in combination with microdialysis in the monkey brain. Brain Res. 849, 85–96.

Psychopharmacology
DOI 10.1007/s00213-011-2633-5

ORIGINAL INVESTIGATION

Striatal and extrastriatal dopamine D_2 receptor occupancy by the partial agonist antipsychotic drug aripiprazole in the human brain: a positron emission tomography study with [^{11}C]raclopride and [^{11}C]FLB457

Keisuke Takahata · Hiroshi Ito · Harumasa Takano · Ryosuke Arakawa · Hironobu Fujiwara · Yasuyuki Kimura · Fumitoshi Kodaka · Takeshi Sasaki · Tsuyoshi Nogami · Masayuki Suzuki · Tomohisa Nagashima · Hitoshi Shimada · Motoichiro Kato · Masaru Mimura · Tetsuya Suhara

Received: 29 October 2011 / Accepted: 26 December 2011

Abstract
Rationale Second-generation antipsychotics demonstrate clinical efficacy with fewer extrapyramidal side effects compared with first-generation antipsychotics. One of the proposed explanations is the hypothesis of preferential extrastriatal dopamine D_2 receptor occupancy (limbic selectivity) by antipsychotics. In the present study, we focused on aripiprazole, which has a unique pharmacological profile with partial agonism at dopamine D_2 receptors and the minimal risk of extrapyramidal side effects. Previous positron emission tomography (PET) studies using high-affinity radioligands for dopamine D_2 receptors have reported inconsistent results regarding regional differences of dopamine D_2 receptor occupancy by aripiprazole.

Objective To test the hypothesis of preferential binding to extrastriatal dopamine D_2 receptors by aripiprazole, we investigated its regional dopamine D_2 receptor occupancies in healthy young subjects.
Materials and methods Using PET and two radioligands with different affinities for dopamine D_2 receptors, [^{11}C]raclopride and [^{11}C]FLB457, striatal and extrastriatal dopamine D_2 receptor bindings at baseline and after oral administration of 6 mg aripiprazole were measured in 11 male healthy subjects.
Results Our data showed that dopamine D_2 receptor occupancies in the striatum measured with [^{11}C]raclopride were 70.1% and 74.1%, with the corresponding values for the extrastriatal regions measured with [^{11}C]FLB457 ranging from 46.6% to 58.4%.
Conclusions In the present study, preferential extrastriatal dopamine D_2 receptor occupancy by aripiprazole was not observed. Our data suggest partial agonism at dopamine D_2 receptors is the most likely explanation for the minimal risk of extrapyramidal side effects in the treatment by aripiprazole.

Keywords Antipsychotics · Dopamine D_2 receptor · Occupancy · Partial agonist · Aripiprazole

K. Takahata · H. Ito · H. Takano · R. Arakawa · H. Fujiwara · Y. Kimura · F. Kodaka · T. Sasaki · T. Nogami · M. Suzuki · T. Nagashima · H. Shimada · T. Suhara
Clinical Neuroimaging Team, Molecular Neuroimaging Program, Molecular Imaging Center, National Institute of Radiological Sciences,
Chiba, Japan

H. Ito (✉)
Biophysics Program, Molecular Imaging Center, National Institute of Radiological Sciences,
4-9-1 Anagawa, Inage-ku,
Chiba 263-8555, Japan
e-mail: hito@nirs.go.jp

K. Takahata · M. Kato · M. Mimura
Department of Neuropsychiatry, Keio University, School of Medicine,
Tokyo, Japan

Introduction

Since the first antipsychotic drug appeared in the mid-twentieth century with the introduction of chlorpromazine, antipsychotic drugs have been the first-line treatment for schizophrenia and related psychotic disorders. Molecular

Published online: 12 January 2012

imaging studies have explored potential pathways to the manifestation of clinical efficacy of various antipsychotics. Past studies revealed that dopamine D_2 receptor occupancy measurements provide a valid predictor of antipsychotic responses and extrapyramidal side effects (Farde et al. 1992; Kapur et al. 2000; Kapur et al. 1999; Nordström et al. 1993).

Second-generation, or atypical, antipsychotics are effective in the treatment of both positive and negative symptoms of schizophrenia. Compared to first-generation antipsychotics, they cause significantly fewer and less severe extrapyramidal side effects and prolactin level elevations (Leucht et al. 2009). Several molecular imaging studies using high-affinity radioligands for dopamine D_2 receptors have reported regional differences of dopamine D_2 receptor occupancy by second-generation antipsychotics. Initially, using [^{123}I]epidepride, Pilowsky et al. (1997) reported "limbic selectivity" of clozapine, i.e., higher dopamine D_2 receptor occupancies in the extrastriatal regions than in the striatum. Similar findings were obtained with clozapine by PET studies using [^{76}Br]FLB457 (Xiberas et al. 2001) and [^{18}F]fallypride (Gründer et al. 2006; Kessler et al. 2006). In contrast, first-generation antipsychotics were reported to show similar dopamine D_2 receptor occupancies in striatal and extrastriatal regions, as measured with [^{123}I]epidepride (Bigliani et al. 1999; Pilowsky et al. 1997). Based on these findings, the hypothesis of the preferential extrastriatal dopamine D_2 receptor occupancy has been suggested to explain the actions of second-generation antipsychotics (Pilowsky et al. 1997). Preferential extrastriatal dopamine D_2 receptor occupancy was also shown in other second-generation antipsychotics, such as risperidone using [^{76}Br]FLB457 (Xiberas et al. 2001) and [^{123}I]epidepride (Bressan et al. 2003), olanzapine using [^{76}Br]FLB457 (Xiberas et al. 2001), and quetiapine using [^{18}F]fallypride (Kessler et al. 2006) in patients with schizophrenia. However, the results of several other molecular imaging studies were inconsistent. For example, studies combining [^{11}C]FLB457 imaging for extrastriatal D_2 receptors and [^{11}C]raclopride imaging for striatal D_2 receptors have reported no differences in occupancy of dopamine D_2 receptors between the striatal and extrastriatal regions in schizophrenia patients taking clozapine (Talvik et al. 2001). The absence of preferential binding to extrastriatal dopamine D_2 receptors was also reported with risperidone (Ito et al. 2009), olanzapine (Arakawa et al. 2010; Kessler et al. 2005), and paliperidone (Arakawa et al. 2007).

In the present study, we focused on aripiprazole, which differs from the above-mentioned first- and second-generation antipsychotics in its unique pharmacological profile. Aripiprazole acts as a partial agonist at dopamine D_2 and serotonin 5-HT_{1A} receptors and as an antagonist at serotonin 5-HT_2 receptors (Burris et al. 2002; Davies et al. 2006). It has been shown to be as effective as haloperidol and risperidone in the treatment of positive and negative symptoms of schizophrenia and schizoaffective disorder. Furthermore, a lower incidence of the known side effects associated with antipsychotics such as extrapyramidal symptoms, weight gain, tardive dyskinesia, prolactin level elevation, and sedation has been observed (Bhattacharjee and El-Sayeh 2008). A PET study using [^{11}C]raclopride reported striatal occupancy values ranging from 60% to 95% without notable extrapyramidal side effects (Yokoi et al. 2002). Preferential extrastriatal dopamine D_2 receptor occupancy by aripiprazole has also been tested in two PET studies using [^{18}F]fallypride in patients diagnosed with schizophrenia (Gründer et al. 2008; Kegeles et al. 2008). Kegeles et al. (2008) reported higher dopamine D_2 receptor occupancies in the extrastriatum compared to the striatum in patients with schizophrenia and schizoaffective disorder treated with aripiprazole. However, in another PET study using the same radioligand, Gründer et al. (2008) reported no regional difference in dopamine D_2 receptor occupancy across brain regions by aripiprazole in 16 patients with schizophrenia or schizoaffective disorder.

The purpose of the present study was to test the hypothesis of preferential binding to extrastriatal dopamine D_2 receptors by aripiprazole. Striatal and extrastriatal dopamine D_2 receptor bindings at baseline and after oral administration of 6 mg aripiprazole were measured using PET in the same healthy subjects. Based on the finding that D_2 receptor densities are quite different between the striatal and extrastriatal regions (Hall et al. 1996; Hall et al. 1994), dopamine D_2 receptor bindings were measured using two radioligands with different affinities—[^{11}C]raclopride for the striatum and [^{11}C]FLB457 for the extrastriatal regions (Farde et al. 1995; Suhara et al. 1999).

Materials and methods

Subjects

The study was approved by the Institutional Review Board of the National Institute of Radiological Sciences, Chiba, Japan. Eleven healthy male subjects [20–35 years, 23.7±4.0 (mean ± S.D.)] participated in the study. Written informed consent was obtained from each subject after complete explanation of the study. Subjects with current or past psychiatric disorders, substance abuse, or organic brain disease were excluded on the basis of their medical history and magnetic resonance (MR) imaging of the brain. Subjects also underwent a physical examination and blood and urine analysis to exclude physical illness.

PET procedures

All PET studies were performed with a Siemens ECAT HR + system, which provides 63 sections with an axial field of view of 15.5 cm (Brix et al. 1997). The intrinsic spatial resolution

was 4.3 mm in-plane and 4.2 mm full-width at half maximum axially. With a Hanning filter (cutoff frequency, 0.4 cycle/pixel), the reconstructed in-plane resolution was 7.5 mm. Data were acquired in three-dimensional mode. Scatter was corrected using the single scatter simulation technique (Watson et al. 1996). Ten-minute transmission scan using a ^{68}Ge–^{68}Ga line source was performed for attenuation correction. A head fixation device with thermoplastic attachments was used to minimize the subject's head movement during the PET measurements.

PET studies were performed under resting condition (baseline study) and with oral administration of aripiprazole (drug challenge study) on separate days. The average interval between baseline studies and drug challenge studies was 15.1± 17.1 days (7–63 days). In each study, the two dynamic PET scans with [^{11}C]raclopride and [^{11}C]FLB457 were performed sequentially. After the intravenous rapid bolus injection of [^{11}C]raclopride, dynamic PET scanning was performed for 60 min. One hour after the end of [^{11}C]raclopride PET measurement, dynamic PET scanning was performed for 90 min after intravenous rapid bolus injection of [^{11}C]FLB457. The frame sequence consisted of 12 20-s frames, 16 1-min frames, and 10 4-min frames for [^{11}C]raclopride, and 9 20-s frames, 5 1-min frames, 4 2-min frames, 11 4-min frames, and 6 5-min frames for [^{11}C]FLB457. The injected radioactivity was 206–235 and 184–240 MBq in baseline studies, and 211–235 and 217–229 MBq in drug challenge studies for [^{11}C]raclopride and [^{11}C]FLB457, respectively. The specific radioactivity was 131–247 and 138–361 GBq/μmol in baseline studies, and 94–270 and 139–277 GBq/μmol in drug challenge studies for [^{11}C]raclopride and [^{11}C]FLB457, respectively. The injected mass was 0.90–1.64 and 0.66–1.34 nmol in baseline studies, and 0.78–2.51 and 0.79–1.73 nmol in drug challenge studies for [^{11}C]raclopride and [^{11}C]FLB457, respectively. Paired t test revealed no significant differences in injected radioactivity, specific radioactivity, and injected mass between baseline and drug challenge studies for both [^{11}C]raclopride and [^{11}C]FLB457.

In the drug challenge study, 6 mg aripiprazole was orally administered 150 min before the start of PET scan with [^{11}C]raclopride. To estimate the plasma concentrations of aripiprazole, venous blood samplings were performed at the start and end of each PET scan. The plasma concentrations of aripiprazole and its main metabolite, dehydroaripiprazole, were determined by the validated liquid chromatography coupled to mass spectrometry/mass spectrometry method (Sumika Chemical Analysis Service Ltd, Tokyo, Japan).

All MR scans were performed with a 3.0-T MR scanner (General Electric, Milwaukee, WI). Three-dimensional volumetric acquisition of T_1-weighted three-dimensional fast-spoiled gradient-recalled acquisition in the steady state (SPGR) sequence produced gapless series of thin transverse sections (TE 2.848 ms; TR 6.992 ms; prep time 900 ms; flip angle 8°; field of view 260 mm; acquisition matrix 256×256; slice thickness 1 mm; scan time 367 s).

Regions of interest

The MR images were co-registered to each of the summation images of all frames of dynamic PET scans for each subject using PMOD (PMOD Technologies Ltd., Zurich, Switzerland). Regions of interest (ROIs) were drawn on the co-registered MR and PET images of each subject: the cerebellum and striatum (caudate head and putamen) for [^{11}C] raclopride studies; the cerebellum and extrastriatum (midbrain, thalamus, parahippocampal gyrus including amygdala, anterior part of the cingulate cortex, frontal cortex, temporal cortex, and parietal cortex) for [^{11}C]FLB457 studies. Each ROI was drawn over three adjacent sections and data were pooled to obtain the average radioactivity concentration for the whole volume of interest. To obtain the regional time–activity curves, the regional radioactivity was calculated for each frame, corrected for decay, and plotted versus time.

Calculation for dopamine D_2 receptor occupancy

For both PET studies with [^{11}C]raclopride and [^{11}C]FLB57, the binding potential (BP_{ND}) was calculated using the simplified reference tissue model method (Lammertsma et al. 1996; Lammertsma and Hume 1996). With this method, the time–activity curve in the target region is described by that in the reference region with no specific binding, assuming that both regions have the same level of non-displaceable radioligand binding:

$$C_t(t) = R_1 C_r(t) + \{k_2 - R_1 k_2/(1 + \mathrm{BP_{ND}})\} \times C_r(t) \otimes \exp\{-k_2 t/(1 + \mathrm{BP_{ND}})\} \quad (1)$$

where $C_t(t)$ is the radioactivity concentration in the target region, $C_r(t)$ is the radioactivity in the reference region, R_1 is the ratio of K_1/K_1' (K_1, influx rate constant for the target brain region; K_1', influx rate constant for the reference region), k_2 is the efflux rate constant for the target region, and ⊗ denotes the convolution integral. In this analysis, three parameters (BP_{ND}, R_1, and k_2) were estimated by nonlinear least-squares curve fitting using PMOD. The cerebellum was used as reference region. Dopamine D_2 receptor occupancy by aripiprazole was calculated as follows:

$$\text{Occupancy}\,(\%) = 100 \times \left(\mathrm{BP_{ND,\,baseline}} - \mathrm{BP_{ND,\,drug}}\right)/\mathrm{BP_{ND,\,baseline}} \quad (2)$$

where $BP_{ND,\,baseline}$ is BP_{ND} in the baseline study, and $BP_{ND,\,drug}$ is BP_{ND} in the drug challenge study.

The relation between the plasma concentration of antipsychotic drug and dopamine D_2 receptor occupancy can be

expressed as follows (Kapur and Remington 1996; Takano et al. 2004):

$$\text{Occupancy}\,(\%) = 100 \times C/(\text{ED}_{50} + C) \quad (3)$$

where C is the plasma concentration of aripiprazole, and ED_{50} is the plasma concentration required to induce 50% occupancy. ED_{50} values for each of the ROIs were calculated using the Prism software system (GraphPad Software Inc., San Diego, CA, USA) to fit the dose–occupancy data for each region, assuming a range from 0% to 100% occupancy.

Anatomic standardization

The analysis using ROIs does not allow evaluation of data throughout the brain. For visualization of regional differences in dopamine D_2 receptor occupancies, intersubject averaging of occupancy images, which requires transformation of brain images of individual subjects into the standard brain shape and size in three dimensions (anatomical standardization), was performed (Fox et al. 1988). BP_{ND} images of [^{11}C] raclopride and [^{11}C] FLB457 were calculated on a voxel-by-voxel basis by the reference tissue model (Lammertsma et al. 1996; Lammertsma and Hume 1996) with the basis function method (Gunn et al. 1997). Images of dopamine D_2 receptor occupancy were also calculated on a voxel-by-voxel basis. All MR images that were co-registered to PET images were transformed into the standard brain size and shape by linear and nonlinear parameters with SPM5 (Wellcome Trust Center for Neuroimaging, Institute of Neurology, London, UK). The brain templates used in SPM5 for the anatomical standardization were T_1 templates for MR images. All BP_{ND} images were also transformed into the standard brain size and shape using the same parameters as MR images. Thus, brain images of all subjects had the same anatomical format. Average images for BP_{ND} and dopamine D_2 receptor occupancy were calculated on a voxel-by-voxel basis.

Statistical analysis

Statistical analyses were performed with SPSS, version 18.0 (SPSS, Inc., Chicago, IL, USA). Paired t tests were performed to compare (1) dopamine D_2 receptor occupancies between the striatal and extrastriatal regions, and (2) plasma concentrations of aripiprazole between [^{11}C]raclopride and [^{11}C]FLB457 PET studies. In all tests, the two-tailed level of statistical significance was set at α=0.05. Multiple comparisons with Bonferroni corrections were performed to test the regional differences of dopamine D_2 receptor occupancies in the extrastriatal regions.

Results

Striatal and extrastriatal BP_{ND} values and dopamine D_2 receptor occupancies are shown in Tables 1 and 2. Dopamine D_2 receptor occupancies in the striatum were 70.1% and 74.1%, and the corresponding values for the extrastriatal regions ranged from 46.6% to 58.4%. Although direct comparison of dopamine D_2 receptor occupancy values between the striatal and extrastriatal regions should be interpreted with some caution due to the small difference of plasma concentration of aripiprazole during the [^{11}C] raclopride and [^{11}C]FLB457 PET studies as well as systematic errors in occupancy for [^{11}C]FLB457 studies as described in the "Discussion", higher dopamine D_2 receptor occupancies in the extrastriatal regions were not observed. No significant difference in dopamine D_2 receptor occupancy was found among the extrastriatal regions by multiple comparison test with Bonferroni corrections.

Average images of BP_{ND} at the baseline condition and after administration of aripiprazole and dopamine D_2 receptor occupancy for [^{11}C]raclopride and [^{11}C]FLB457 are shown in Figs. 1 and 2, respectively. Intersubject averaging of images allowed visualization of regional differences in dopamine D_2 receptor occupancy throughout the brain. Dopamine D_2 receptor occupancy by aripiprazole was almost uniform among the cerebral cortices.

The plasma concentrations of aripiprazole and dehydroaripiprazole in [^{11}C]raclopride PET studies averaged between the start and end of each scanning were 29.4±4.8 and 1.4±0.6 ng/ml (mean ± S.D.), and the corresponding values in [^{11}C]FLB457 PET studies were 25.6±2.2 and 1.7± 0.7 ng/ml (mean ± S.D.), respectively. The plasma concentration of aripiprazole in the [^{11}C]raclopride studies was higher than that in the [^{11}C]FLB457 studies (p<0.01). We generated dose–occupancy curves as described in the "Methods" section for each of the nine regions analyzed, yielding the ED_{50} value for each region. The ED_{50} values were 9.9 ng/ml for the striatum (r=0.40 for curve fitting), 12.2 ng/ml for the putamen (r=0.58), 29.4 ng/ml for the midbrain (r=0.36), 24.4 ng/ml for the parahippocampal gyrus (r=0.15), 18.9 ng/ml for the thalamus (r=0.50), 24.1 ng/ml for the anterior cingulate gyrus (r=0.29),

Table 1 Striatal binding potential (BP_{ND}) values and dopamine D_2 receptor occupancy in [^{11}C] raclopride PET studies

Region	BP_{ND}		Occupancy (%)
	Baseline	Drug challenge	
Caudate head	2.55±0.28	0.66±0.19	74.1±6.7
Putamen	3.52±0.30	1.04±0.18	70.1±6.3

Values are mean ± S.D.

Table 2 Extrastriatal binding potential (BP_{ND}) values and dopamine D_2 receptor occupancy in [^{11}C]FLB457 PET studies

Region	BP_{ND}		Occupancy (%)
	Baseline	Drug challenge	
Midbrain	1.78±0.41	0.94±0.23	46.6±9.9
Thalamus	4.30±0.63	1.81±0.29	57.6±6.7
Parahippocampal gyrus	1.87±0.34	0.89±0.17	51.2±10.7
Anterior cingulate	1.15±0.17	0.53±0.12	51.5±6.6
Frontal cortex	1.06±0.20	0.52±0.12	51.3±9.2
Temporal cortex	1.83±0.29	0.76±0.11	58.4±3.0
Parietal cortex	1.20±0.25	0.53±0.13	55.6±4.8

Values are mean ± S.D.

24.3 ng/ml for the frontal cortex (r=0.25), 18.2 ng/ml for the temporal cortex (r=0.35), and 20.4 ng/ml for the parietal cortex (r=0.21).

Discussion

To test the hypothesis of preferential extrastriatal dopamine D_2 receptor binding by aripiprazole, we performed PET examinations using [^{11}C] raclopride and [^{11}C] FLB457 in healthy subjects. The preferential extrastriatal dopamine D_2 receptor occupancy by aripiprazole was not observed in this study.

PET examinations using [^{11}C]raclopride and [^{11}C]FLB457 in the present study showed higher dopamine D_2 receptor occupancy in the [^{11}C]raclopride studies than in the [^{11}C] FLB457 studies, and therefore lower ED_{50} values were observed in the striatum compared to those in the extrastriatal regions. Two possible sources for these differences should be considered on the basis of our previous simulation study of regional dopamine D_2 receptor occupancies using the identical multiple radioligand method. First, the effects of small but non-negligible specific binding in the cerebellum in [^{11}C] FLB457 PET studies need to be taken into account. We previously showed that non-negligible specific binding in the cerebellum can cause an underestimation of about 8% in dopamine D_2 receptor occupancy measured by [^{11}C]FLB457 PET when BP_{ND} in the cerebellum was 0.3 and assumed occupancy without consideration of specific binding in the cerebellum was 70% (Ito et al. 2001; Ito et al. 2008). This indicated that the occupancies of dopamine D_2 receptors by aripiprazole in the striatum would not be different from those in the extrastriatal regions. Another possible source for the difference in dopamine D_2 receptor occupancy between striatal and extrastriatal regions is related to the time point of the scan and plasma concentrations of aripiprazole. In the present study, [^{11}C]FLB457 PET studies began 2 h after the start of [^{11}C]raclopride PET studies, and therefore the plasma concentration of aripiprazole was slightly lower during [^{11}C]FLB457 studies (25.6±2.2 ng/ml) than during [^{11}C]raclopride PET studies (29.4±4.8 ng/ml). When ED_{50} was considered to be 10 ng/ml, 29.4 and 25.6 ng/ml of the plasma concentrations of aripiprazole were estimated to yield 75% and 72% of dopamine D_2 receptor occupancy, respectively (Eq. 3). This might also partially explain the higher dopamine D_2 receptor occupancies in [^{11}C]raclopride studies than in [^{11}C]FLB457 studies. Taken together, it is concluded that aripiprazole

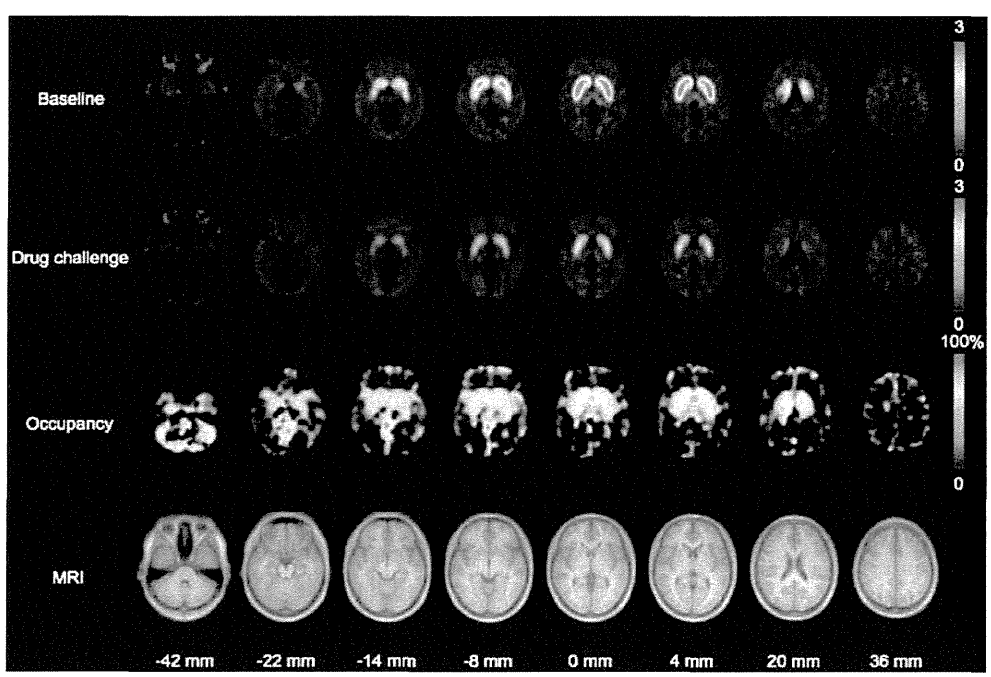

Fig. 1 Average images of binding potential at baseline condition and after administration of aripiprazole, dopamine D_2 receptor occupancy for [^{11}C]raclopride, and T_1-weighted images. In the striatum, no obvious regional differences in dopamine D_2 receptor occupancy were observed

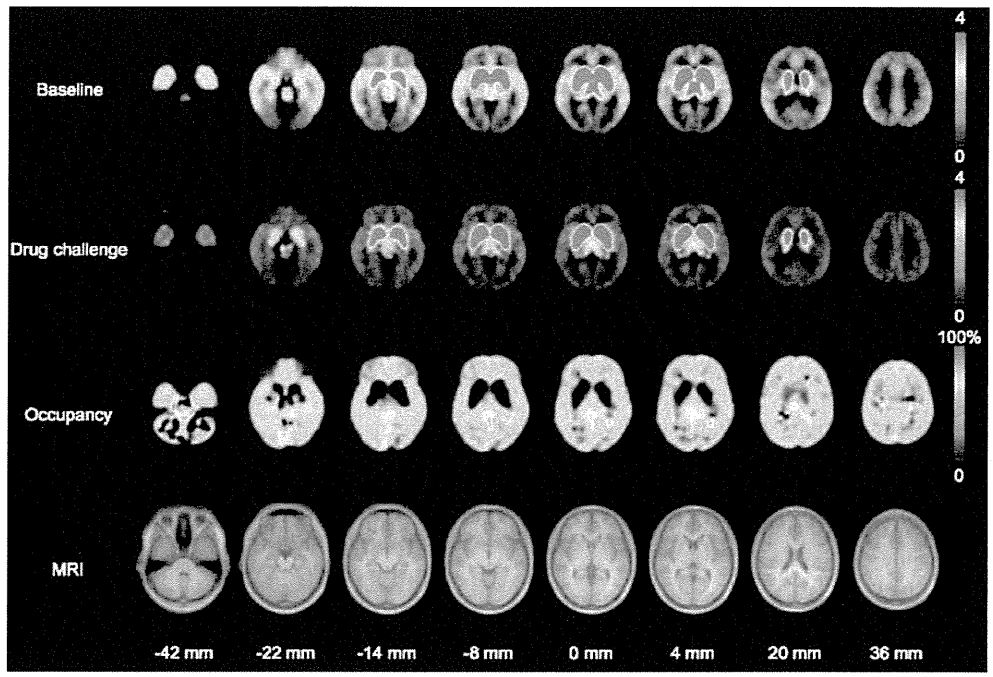

Fig. 2 Average images of binding potential at baseline condition and after administration of aripiprazole, dopamine D_2 receptor occupancy for [^{11}C]FLB457, and T_1-weighted images. Among extrastriatal regions, no obvious regional differences in dopamine D_2 receptor occupancy were observed. Note that dopamine D_2 receptor occupancies in the striatum could not be calculated correctly in [^{11}C]FLB457 studies due to the extremely high BP_{ND} values. Therefore, BP_{ND} values higher than 10.0 were cut off from average images, and this accounts for the striatum appearing to have zero occupancy values

demonstrates similar dopamine D_2 receptor occupancies in the striatal and extrastriatal regions.

Aripiprazole is an antipsychotic drug with high affinity for dopamine D_2 receptors (Davies et al. 2006). Past clinical studies have shown that aripiprazole demonstrates clinical efficacy equal to first-generation antipsychotics but with a lower risk of extrapyramidal side effects (Bhattacharjee and El-Sayeh 2008). To explain the clinical properties of aripiprazole, two hypotheses have been proposed. First, it has been assumed that aripiprazole as a partial agonist exhibits an intrinsic activity at dopamine D_2 receptors (Lawler et al. 1999). Therefore, it is theoretically possible that even at 90% receptor occupancy by aripiprazole, extrapyramidal side effects comparable to those expected with first-generation antipsychotics do not occur. Second, preferential extrastriatal dopamine D_2 receptor binding has been proposed as a possible mechanism of second-generation antipsychotics and aripiprazole. However, previous PET studies using [^{18}F]fallypride, where regional differences of dopamine D_2 receptor occupancy by aripiprazole were investigated in patients with schizophrenia, reported inconsistent conclusions. Kegeles et al. (2008) reported higher dopamine D_2 receptor occupancies in the extrastriatal regions compared to the striatum in patients with schizophrenia and schizoaffective disorder treated with aripiprazole. Another PET study using [^{18}F]fallypride was in agreement in showing relatively higher ED_{50} values in the striatum than those in the extrastriatal regions but reported no significant regional difference in dopamine D_2 receptor occupancy across brain regions by aripiprazole in patients with schizophrenia or schizoaffective disorder (Gründer et al. 2008). Since those two PET studies differed in scan durations, subject groups at baseline, and drug challenge studies, it was possible that these methodological differences caused different results. In the present study, preferential extrastriatal dopamine D_2 receptor occupancy was not observed by the multiple radioligands method. Thus, partial agonism at dopamine D_2 receptors is the most likely explanation for the minimal risk of extrapyramidal side effects in the treatment by aripiprazole.

There are several methodological issues to be discussed. While previous studies measured dopamine D_2 receptor occupancies in the striatal and extrastriatal regions using a single high-affinity radioligand, we used [^{11}C] raclopride and [^{11}C] FLB457 for the striatal and extrastriatal regions, respectively. Since dopamine D_2 receptor densities are quite different between the striatal and extrastriatal regions (Hall et al. 1996; Hall et al. 1994), different radioligands with different affinities for dopamine D_2 receptors have been shown to be preferable (Olsson and Farde 2001). It has also been pointed out that insufficient scan durations in PET studies with a single high-affinity radioligand could cause the underestimation of BP_{ND} values especially in regions with high dopamine D_2 receptor densities due to a failure of reaching equilibrium (Ito et al. 2009; Olsson and Farde 2001). Although previous studies indicated that too short data acquisition time in [^{11}C] FLB457 PET studies could cause the underestimation of occupancy in the extrastriatal regions (Erlandsson et al. 2003), the accuracy of the estimation of extrastriatal BP_{ND} and occupancy in [^{11}C]FLB457 studies with a data acquisition time over 60 min has been confirmed (Ito et al. 2001; Olsson and Farde 2001; Sudo et al. 2001). Accuracy of the estimation of striatal BP_{ND} using [^{11}C]raclopride was also confirmed (Ito et al. 1998; Lammertsma et al. 1996). In the present study, we

did not randomize the order of the two PET scans with [^{11}C] raclopride and [^{11}C]FLB457. Since washout from the brain with [^{11}C]raclopride is faster than that with [^{11}C]FLB457, we performed PET scans with [^{11}C]raclopride before those with [^{11}C]FLB457. This could be a potential limitation because the plasma concentration of aripiprazole at the time of two PET scans significantly differed, as mentioned above.

To calculate dopamine D_2 receptor occupancies, we used the subject's own baseline data to determine dopamine D_2 receptor occupancies by aripiprazole. Although previous studies showed little or no difference in dopamine D_2 receptor density in the striatum (Farde et al. 1990) or in the extrastriatal regions (Suhara et al. 2002) between normal subjects and patients with schizophrenia, individual differences in dopamine D_2 receptor density might potentially lead to an error in the estimation of dopamine D_2 receptor occupancy (Farde et al. 1992).

The administered dose of aripiprazole for measuring dopamine D_2 receptor occupancies should also be considered. Aripiprazole treatment has been shown to be well tolerated across a range of previously studied doses (2–30 mg/day) (Bhattacharjee and El-Sayeh 2008). In Japan, the starting dose of aripiprazole was set at 6–12 mg/day, and the recommended daily dose ranging from 6 to 24 mg/day in patients with schizophrenia was confirmed (Ohmori et al. 2006). From an ethical standpoint, a relatively small dose of aripiprazole (6 mg) was administered in the present study, and lower plasma concentrations and dopamine D_2 receptor occupancies were observed compared to the past studies. Since it has been proposed that compounds with a long plasma half-life and/or a high affinity are described by a steep curve in dose–occupancy relationship (Gründer et al. 2008), the single-dose setting and the relatively small dose of aripiprazole in the present study might have been a limitation in the calculation of ED_{50}. Thus, whether aripiprazole has different striatal and extrastriatal occupancies at lower/higher doses remains unclear in the present study. In a future study, administration of lower/higher doses of aripiprazole should be tested in the measurement of dopamine D_2 receptor occupancies to calculate accurate ED_{50} at a wider range of plasma concentrations.

Acknowledgments This study was supported in part by a Grant-in-Aid for the Molecular Imaging Program from the Ministry of Education, Culture, Sports, Science and Technology, Japanese Government. We thank Mr. Katsuyuki Tanimoto and Mr. Takahiro Shiraishi for their assistance in performing the PET experiments, Ms. Kazuko Suzuki and Ms. Izumi Izumida for their help as clinical research coordinators, Dr. Takaaki Mori, Dr. Hajime Fukuda and Ms. Yoko Eguchi for their clinical support, and Ms. Mika Omatsu and Ms. Rie Inagaki for their help in performing MRI scanning.

Statement of interest The authors declare that no financial support or compensation has been received from any individual or corporate entity for research or professional service, and there is no personal financial holding that could be perceived as constituting a potential conflict of interest.

References

Arakawa R, Ito H, Takano A, Takahashi H, Morimoto T, Sassa T, Ohta K, Kato M, Okubo Y, Suhara T (2007) Dose-finding study of paliperidone ER based on striatal and extrastriatal dopamine D_2 receptor occupancy in patients with schizophrenia. Psychopharmacology 197:229–235

Arakawa R, Ito H, Okumura M, Takano A, Takahashi H, Takano H, Okubo Y, Suhara T (2010) Extrastriatal dopamine D_2 receptor occupancy in olanzapine-treated patients with schizophrenia. Eur Arch Psychiatry Clin Neurosci 260:345–350

Bhattacharjee J, El-Sayeh HGG (2008) Aripiprazole versus typical antipsychotic drugs for schizophrenia. Cochrane Database of Systematic Reviews: CD006617

Bigliani V, Mulligan RS, Acton PD, Visvikis D, Ell PJ, Stephenson C, Kerwin RW, Pilowsky LS (1999) In vivo occupancy of striatal and temporal cortical D_2/D_3 dopamine receptors by typical antipsychotic drugs. [^{123}I]epidepride single photon emission tomography (SPECT) study. Br J Psychiatry 175:231–238

Bressan RA, Erlandsson K, Jones HM, Mulligan RS, Ell PJ, Pilowsky LS (2003) Optimizing limbic selective D_2/D_3 receptor occupancy by risperidone: a [^{123}I]-epidepride SPET study. J Clin Psychopharmacol 23:5–14

Brix G, Zaers J, Adam LE, Bellemann ME, Ostertag H, Trojan H, Haberkorn U, Doll J, Oberdorfer F, Lorenz WJ (1997) Performance evaluation of a whole-body PET scanner using the NEMA protocol. J Nucl Med 38:1614–1623

Burris KD, Molski T, Xu C, Ryan E, Tottori K, Kikuchi T, Yocca F, Molinoff P (2002) Aripiprazole, a novel antipsychotic, is a high-affinity partial agonist at human dopamine D_2 receptors. J Pharmacol Exp Ther 302:381–389

Davies MA, Sheffler DJ, Roth BL (2006) Aripiprazole: a novel atypical antipsychotic drug with a uniquely robust pharmacology. CNS Drug Rev 10:317–336

Erlandsson K, Bressan RA, Mulligan RS, Ell PJ, Cunningham VJ, Pilowsky LS (2003) Analysis of D_2 dopamine receptor occupancy with quantitative SPET using the high-affinity ligand [^{123}I]epidepride: resolving conflicting findings. Neuroimage 19:1205–1214

Farde L, Wiesel FA, Stone-Elander S, Halldin C, Nordström AL, Hall H, Sedvall G (1990) D2 dopamine receptors in neuroleptic-naive schizophrenic patients. A positron emission tomography study with [11 C]raclopride. Arch Gen Psychiatry 47:213–219

Farde L, Nordström AL, Wiesel FA, Pauli S, Halldin C, Sedvall G (1992) Positron emission tomographic analysis of central D_1 and D_2 dopamine receptor occupancy in patients treated with classical neuroleptics and clozapine. Relation to extrapyramidal side effects. Arch Gen Psychiatry 49:538–544

Farde L, Hall H, Pauli S, Halldin C (1995) Variability in D_2-dopamine receptor density and affinity: a PET study with [^{11}C]raclopride in man. Synapse 20:200–208

Fox PT, Mintun MA, Reiman EM, Raichle ME (1988) Enhanced detection of focal brain responses using intersubject averaging and change-distribution analysis of subtracted PET images. J Cereb Blood Flow Metab 8:642–653

Gründer G, Landvogt C, Vernaleken I, Buchholz H-G, Ondracek J, Siessmeier T, Härtter S, Schreckenberger M, Stoeter P, Hiemke C, Rösch F, Wong DF, Bartenstein P (2006) The striatal and extrastriatal D2/D3 receptor-binding profile of clozapine in patients with schizophrenia. Neuropsychopharmacology 31:1027–1035

Gründer G, Fellows C, Janouschek H, Veselinovic T, Boy C, Bröcheler A, Kirschbaum KM, Hellmann S, Spreckelmeyer KM, Hiemke C, Rösch F, Schaefer WM, Vernaleken I (2008) Brain and plasma

pharmacokinetics of aripiprazole in patients with schizophrenia: an [^{18}F]fallypride PET study. Am J Psychiatry 165:988–995

Gunn RN, Lammertsma AA, Hume SP, Cunningham VJ (1997) Parametric imaging of ligand-receptor binding in PET using a simplified reference region model. Neuroimage 6:279–287

Hall H, Sedvall G, Magnusson O, Kopp J, Halldin C, Farde L (1994) Distribution of D_1- and D_2-dopamine receptors, and dopamine and its metabolites in the human brain. Neuropsychopharmacology 11:245–256

Hall H, Farde L, Halldin C, Hurd Y, Pauli S (1996) Autoradiographic localization of extrastriatal D_2–dopamine receptors in the human brain using [^{125}I] epidepride. Synapse 23:115–123

Ito H, Hietala J, Blomqvist G, Halldin C, Farde L (1998) Comparison of the transient equilibrium and continuous infusion method for quantitative PET analysis of [^{11}C]raclopride binding. J Cereb Blood Flow Metab 18:941–950

Ito H, Sudo Y, Suhara T, Okubo Y, Halldin C, Farde L (2001) Error Analysis for quantification of [^{11}C]FLB 457 binding to extrastriatal D_2 dopamine receptors in the human brain. Neuroimage 13:531–539

Ito H, Takahashi H, Arakawa R, Takano H, Suhara T (2008) Normal database of dopaminergic neurotransmission system in human brain measured by positron emission tomography. Neuroimage 39:555–565

Ito H, Arakawa R, Takahashi H, Takano H, Okumura M, Otsuka T, Ikoma Y, Shidahara M, Suhara T (2009) No regional difference in dopamine D_2 receptor occupancy by the second-generation antipsychotic drug risperidone in humans: a positron emission tomography study. Int J Neuropsychopharmacol 12:667–675

Kapur S, Remington G (1996) Serotonin–dopamine interaction and its relevance to schizophrenia. Am J Psychiatry 153:466–476

Kapur S, Zipursky RB, Remington G (1999) Clinical and theoretical implications of 5-HT_2 and D_2 receptor occupancy of clozapine, risperidone, and olanzapine in schizophrenia. Am J Psychiatry 156:286–293

Kapur S, Zipursky R, Jones C, Remington G, Houle S (2000) Relationship between dopamine D_2 occupancy, clinical response, and side effects: a double-blind PET study of first-episode schizophrenia. Am J Psychiatry 157:514–520

Kegeles LS, Slifstein M, Frankle WG, Xu X, Hackett E, Bae S-A, Gonzales R, Kim J-H, Alvarez B, Gil R, Laruelle M, Abi-Dargham A (2008) Dose–occupancy study of striatal and extrastriatal dopamine D_2 receptors by aripiprazole in schizophrenia with PET and [^{18}F]Fallypride. Neuropsychopharmacology 33:3111–3125

Kessler RM, Ansari MS, Riccardi P, Li R, Jayathilake K, Dawant B, Meltzer HY (2005) Occupancy of striatal and extrastriatal dopamine D_2/D_3 receptors by olanzapine and haloperidol. Neuropsychopharmacology 30:2283–2289

Kessler RM, Ansari MS, Riccardi P, Li R, Jayathilake K, Dawant B, Meltzer HY (2006) Occupancy of striatal and extrastriatal dopamine D_2 receptors by clozapine and quetiapine. Neuropsychopharmacology 31:1991–2001

Lammertsma AA, Hume SP (1996) Simplified reference tissue model for PET receptor studies. Neuroimage 4:153–158

Lammertsma AA, Bench CJ, Hume SP, Osman S, Gunn K, Brooks DJ, Frackowiak RS (1996) Comparison of methods for analysis of clinical [^{11}C]raclopride studies. J Cereb Blood Flow Metab 16:42–52

Lawler CP, Prioleau C, Lewis MM, Mak C, Jiang D, Schetz JA, Gonzalez AM, Sibley DR, Mailman RB (1999) Interactions of the novel antipsychotic aripiprazole (OPC-14597) with dopamine and serotonin receptor subtypes. Neuropsychopharmacology 20:612–627

Leucht S, Corves C, Arbter D, Engel RR, Li C, Davis JM (2009) Second-generation versus first-generation antipsychotic drugs for schizophrenia: a meta-analysis. Lancet 373:31–41

Nordström AL, Farde L, Wiesel FA, Forslund K, Pauli S, Halldin C, Uppfeldt G (1993) Central D2-dopamine receptor occupancy in relation to antipsychotic drug effects: a double-blind PET study of schizophrenic patients. Biol Psychiatry 33:227–235

Ohmori T, Miura S, Yamashita I, Koyama T, Yu M, Yagi G, Murasaki M, Kudo Y, Sakai T, Saito M, Watanabe M, Nakane M (2006) Long-term study to examine the efficacy and safety of aripiprazole for schizophrenia—extended study from a late phase II study. Jpn J Clin Psychopharmacol 9:453–474

Olsson H, Farde L (2001) Potentials and pitfalls using high affinity radioligands in PET and SPET determinations on regional drug induced D2 receptor occupancy—a simulation study based on experimental data. Neuroimage 14:936–945

Pilowsky LS, Mulligan RS, Acton PD, Ell PJ, Costa DC, Kerwin RW (1997) Limbic selectivity of clozapine. Lancet 350:490–491

Sudo Y, Suhara T, Inoue M, Ito H, Suzuki K, Saijo T, Halldin C, Farde L (2001) Reproducibility of [^{11}C]FLB 457 binding in extrastriatal regions. Nucl Med Commun 22:1215–1221

Suhara T, Sudo Y, Okauchi T, Maeda J, Kawabe K, Suzuki K, Okubo Y, Nakashima Y, Ito H, Tanada S, Halldin C, Farde L (1999) Extrastriatal dopamine D2 receptor density and affinity in the human brain measured by 3D PET. Int J Neuropsychopharmacol 2:73–82

Suhara T, Okubo Y, Yasuno F, Sudo Y, Inoue M, Ichimiya T, Nakashima Y, Nakayama K, Tanada S, Suzuki K, Halldin C, Farde L (2002) Decreased dopamine D_2 receptor binding in the anterior cingulate cortex in schizophrenia. Arch Gen Psychiatry 59:25–30

Takano A, Suhara T, Ikoma Y, Yasuno F, Maeda J, Ichimiya T, Sudo Y, Inoue M, Okubo Y (2004) Estimation of the time-course of dopamine D_2 receptor occupancy in living human brain from plasma pharmacokinetics of antipsychotics. Int J Neuropsychopharmacol 7:19–26

Talvik M, Nordström A, Nyberg S (2001) No support for regional selectivity in clozapine-treated patients: a PET study with [^{11}C] raclopride and [^{11}C] FLB 457. Am J Psychiatry 158:926–930

Watson C, Newport D, Casey M (1996) A single scatter simulation technique for scatter correction in 3D PET. In: Grangeat P, Amans J-L (eds) Three-dimensional image reconstruction in radiology and nuclear medicine. Kluwer Academic, Dordrecht, pp 255–268

Xiberas X, Martinot JL, Mallet L, Artiges E, Loc HC, Mazière B, Paillère-Martinot ML (2001) Extrastriatal and striatal D2 dopamine receptor blockade with haloperidol or new antipsychotic drugs in patients with schizophrenia. Br J Psychiatry 179:503–508

Yokoi F, Gründer G, Biziere K, Stephane M, Dogan AS, Dannals RF, Ravert H, Suri A, Bramer S, Wong DF (2002) Dopamine D_2 and D_3 receptor occupancy in normal humans treated with the antipsychotic drug aripiprazole (OPC 14597): a study using positron emission tomography and [^{11}C]raclopride. Neuropsychopharmacology 27:248–259

SYNAPSE 65:624–633 (2011)

Serotonergic Neurotransmission in the Living Human Brain: A Positron Emission Tomography Study Using [^{11}C]DASB and [^{11}C]WAY100635 in Young Healthy Men

HARUMASA TAKANO,[1]* HIROSHI ITO,[1] HIDEHIKO TAKAHASHI,[1] RYOSUKE ARAKAWA,[1] MASAKI OKUMURA,[1] FUMITOSHI KODAKA,[1] TATSUI OTSUKA,[1] MOTOICHIRO KATO,[2] AND TETSUYA SUHARA[1]

[1]*Department of Molecular Neuroimaging, Molecular Imaging Center, National Institute of Radiological Sciences, Chiba 263-8555, Japan*

[2]*Department of Neuropsychiatry, Keio University School of Medicine, Shinjuku-ku, Tokyo 160-8582, Japan*

KEY WORDS normal database; serotonin; serotonin transporter; serotonin 1A receptor; positron emission tomography

ABSTRACT The central serotonergic (5-HT) system is closely involved in regulating various mental functions such as mood and emotion. In this system, the serotonin transporter (5-HTT) and the 5-HT_{1A} receptor play important roles in the pathophysiology and treatment of mood and anxiety disorders. However, only a few integrated databases have considered the intraindividual relationship between pre- and postsynaptic serotonergic transmission. In the present study, we constructed a database of 5-HTT and 5-HT_{1A} receptors using positron emission tomography (PET) with [^{11}C]DASB and [^{11}C]WAY100635, respectively. Seventeen healthy young men participated in this study. After anatomic standardization of original images, BP_{ND} was calculated on a voxel-by-voxel basis using reference tissue methods. The highest binding to 5-HTT was observed in the dorsal raphe nucleus, striatum, and thalamus; moderate binding, in the insula and cingulate cortex; and very low binding, in the cerebral neocortex. In contrast, the highest binding to 5-HT_{1A} receptors was seen in the hippocampal regions, insula, neocortical regions, and dorsal raphe nucleus, and very low binding was found in the thalamus and basal ganglia. These distribution patterns were in agreement with those reported in human postmortem studies and previous PET investigations. In addition, exploratory analysis indicated significant negative correlations between the BP_{ND} values with both radiotracers in certain regions of the brain, such as the cingulate, insula, and frontal, temporal and parietal cortices (Pearson's correlation, $P < 0.05$). These databases facilitate the understanding of the regional distribution of serotonergic neurotransmission function in the living human brain and the pathophysiology of various neuropsychiatric disorders. **Synapse 65:624–633, 2011.**

INTRODUCTION

The central serotonergic (5-hydroxytryptamine, 5-HT) system is one of the major neurotransmitters in the brain and is intricately involved in the regulation of various mental functions such as emotion and cognition. Therefore, dysregulation of this system has been implicated in a variety of neuropsychiatric conditions including mood and anxiety disorders, schizophrenia, etc. (Cooper et al., 2002; Nestler et al., 2008).

To date, seven distinct families (5-HT_1-5-HT_7) and at least 16 subtypes of 5-HT receptors and a serotonin transporter (5-HTT) have been identified (Hoyer et al., 2002; Kitson, 2007). Each subtype has distinct functions, and their distributions in the brain are heterogeneous. Many attempts have been made to develop suita-

Contract grant sponsors: Grant-in-Aid for Molecular Imaging Program from the Ministry of Education, Culture, Sports and Technology (MEXT), Japanese Government and a Grant-in-Aid for Scientific Research (C) from the Japan Society for the Promotion of Science; Contract grant number: 20591382

*Correspondence to: Harumasa Takano, Molecular Neuroimaging Group, Molecular Imaging Center, National Institute of Radiological Sciences, 4-9-1 Anagawa, Inage-ku, Chiba, 263-8555, Japan. E-mail: hrtakano@nirs.go.jp

Received 27 September 2010; Accepted 10 November 2010

DOI 10.1002/syn.20883

Published online 23 November 2010 in Wiley Online Library (wileyonlinelibrary.com).

ble radiotracers to visualize and quantify central serotonergic transmission in the living human brain by using PET and single photon emission computed tomography (SPECT) (Brust et al., 2006; Kumar and Mann, 2007; Meyer, 2007; Moresco et al., 2006). In the serotonergic system, only 5-HTT, 5-HT_{1A}, 5-HT_{2A}, and 5-HT_4 receptors and 5-HT synthesis have been visualized in living human brain because of the limited availability of radioligands for humans, although a few have been under development (Diksic and Young, 2001; Lundquist et al., 2006; Marner et al., 2009; Moresco et al., 2006).

The 5-HTT is responsible for the reuptake of 5-HT from the synaptic cleft and the modulation of its extracellular concentration. Therefore, 5-HTT is the primary target molecule of selective serotonin reuptake inhibitors (SSRIs), the most commonly used antidepressants today (Brust et al., 2006; Meyer, 2007). In contrast, the 5-HT_{1A} receptor is localized as a somatodendritic autoreceptor in the dorsal raphe nuclei and as a postsynaptic receptor in the cortical and limbic serotonin terminal fields throughout the brain. The 5-HT_{1A} autoreceptor in the dorsal raphe controls the firing of general 5-HT transmission. In addition, it is the target of 5-HT_{1A} agonists such as buspirone and tandospirone, which have anxiolytic properties. Therefore, both serotonergic functions have been reported to be closely involved in various neuropsychiatric conditions including mood and anxiety disorders, schizophrenia, etc. [see reviews, e.g., (Brust et al., 2006; Drevets et al., 2007; Kumar and Mann, 2007; Savitz et al., 2009; Stockmeier, 2003)].

Recently, we created a normal database for the dopaminergic neurotransmission system by studying healthy volunteers and using five different PET radiotracers, although different cohorts were used for each tracer (Ito et al., 2008). We discussed anatomic localization of receptors and transporters compared with the results of human postmortem studies using autoradiography. In contrast, there has been little integrated database information regarding normal serotonergic transmission, particularly using multiple radioligands to examine both pre- and postsynaptic serotonergic function in the same individuals (Lundberg et al., 2007). In the present study, we conducted two PET scans for each subject using [^{11}C]DASB and [^{11}C]WAY100635 for 5-HTT and 5-HT_{1A} receptor imaging, respectively. We generated parametric images with anatomic standardization of 5-HTT and 5-HT_{1A} binding and subsequently examined the neuroanatomical localization for inter- and intrasubject comparisons.

MATERIALS AND METHODS

Subjects

This study was approved by the Ethics and Radiation Safety Committee of the National Institute of Radiological Sciences, Chiba, Japan. Seventeen healthy men aged 24.4 ± 5.9 (mean ± standard deviation, (SD); range 20–40) years were recruited. All subjects gave their informed written consent before participating in the study. Based on their medical history and an unstructured examination by psychiatrists, the subjects were found to be free of somatic, neurological, and psychiatric disorders. All participants were nonsmokers. The participants had no history of current or previous drug abuse and had not taken any drugs within 2 weeks before the PET studies. The duration between the two PET scans was 7.2 ± 8.7 (range, 0–28) days.

All participants underwent magnetic resonance imaging (MRI) of the brain with a 1.5T MR scanner (Philips Medical Systems, Best, The Netherlands). Three-dimensional volumetric acquisition of a T1-weighted gradient echo sequence produced a gapless series of thin transverse sections (TE: 9.2 msec; TR: 21 msec; flip angle: 30°; field of view: 256 mm; acquisition matrix: 256 × 256; slice thickness: 1 mm). The MRI results revealed no apparent structural abnormalities.

PET procedure

All PET studies were performed with a Siemens ECAT Exact HR+ system (CTI-Siemens, Knoxville, TN), which provides 63 sections with an axial field of view of 15.5 cm. The intrinsic spatial resolution was 4.3 mm in-plane and 4.2 mm full-width at half-maximum (FWHM) axially. With a Hanning filter (cutoff frequency: 0.4 cycle/pixel), the reconstructed in-plane resolution was 7.5 mm FWHM. Data were acquired in three-dimensional mode for [^{11}C]WAY100635 and in two-dimensional mode for [^{11}C]DASB, since [^{11}C]DASB is substantially trapped at first pass through human lungs because of the high expression of 5-HTT on the pulmonary membrane, leading to excessive random counts from three-dimensional head recordings (Suhara et al., 1998). Scatter was corrected for the three-dimensional mode (Watson et al., 1996). A head-fixation device with thermoplastic attachments (Fixster Instruments, Stockholm, Sweden) for individual fit minimized head movement during PET measurements. A 10-min transmission scan using a ^{68}Ge-^{68}Ga line source was performed in order to correct for attenuation. After an i.v. bolus injection of [^{11}C]WAY100635 or [^{11}C]DASB, data were acquired for 90 min in a consecutive series of time frames. The frame sequence consisted of nine 20-s frames, five 1-min frames, four 2-min frames, eleven 4-min frames, and six 5-min frames for [^{11}C]DASB; and twelve 20-s frames, sixteen 1-min frames, ten 4-min frames, and five 6-min frames for [^{11}C]WAY100635. Injected radioactivity was 749.7 ± 37.4 MBq and 224.8 ± 9.1 MBq for [^{11}C]DASB and [^{11}C]WAY100635, respectively. Specific radioactivity was 281.7 ± 92.7 GBq/μmol and

153.9 ± 61.8 GBq/μmol at the time of injection for [^{11}C]DASB and [^{11}C]WAY100635, respectively.

Preprocessing

A PET summation image of all frames and dynamic images were coregistered to each individual MR image by using PMOD (PMOD Technologies, Zurich, Switzerland). The individual MR image was spatially normalized to the Montreal Neurological Institute (MNI) stereotaxic brain, and subsequently, the transformation parameters were applied to the coregistered PET dynamic images. Thus, the PET and MR images of all subjects were anatomically standardized to the MNI template. Volumes of interest (VOIs) were manually delineated by a rater (H.T.) in the cerebellar cortex, dorsal raphe nuclei, thalamus, and striatum for [^{11}C]DASB, and in the cerebellar cortex and hippocampal area for [^{11}C]WAY100635, on the averaged and standardized PET summation and MR images by using the PMOD fusion tool. Circular VOIs with a diameter of 8 mm in the transaxial planes were set for the dorsal raphe nucleus from $z = -38$ to $z = -30$ in the coordinate of the MNI template. To obtain regional time-activity curves, regional radioactivity was calculated for each time frame, corrected for decay and plotted versus time.

Calculation of binding potentials and generation of parametric images for both tracers

For the PET study with [^{11}C]WAY100635, the binding potential (BP) for nondisplaceable radioligand in tissue (BP_{ND}) (Innis et al., 2007) was calculated using a reference tissue model on a voxel-by-voxel basis (Lammertsma and Hume, 1996).

$$C_T(t) = R_1 C_R(t) + \left(k_2 - \frac{R_1 k_2}{1 + BP_{ND}}\right) C_R(t) \otimes \exp\left(\frac{-k_2 t}{1 + BP_{ND}}\right),$$

where $C_T(t)$ is the radioactivity concentration in a brain region, and $C_R(t)$ is the radioactivity concentration in the reference region. R_1 is the ratio of K_1/K_1' (K_1, influx rate constant for the brain region, K_1', influx rate constant for the reference region), k_2 is the efflux rate constant for the brain region, and $\otimes$ denotes the convolution integral. In this analysis, three parameters (BP_{ND}, R_1, and k_2) were estimated by the basis function method (Gunn et al., 1997, 1998). The cerebellum was used as reference region because a postmortem study indicated that the cerebellum cortex is almost devoid of 5-HT_{1A} receptors (Varnas et al., 2004).

For the PET study with [^{11}C]DASB, BP_{ND} was calculated by using a multi-linear reference tissue model 2 (MRTM2) (Ichise et al., 2003),

$$C_T(T) = -\frac{V}{V'b}\left(\int_0^T C_R(t)dt + \frac{1}{k_2'} C_R(t)\right) + \frac{1}{b}\int_0^T C_T(t)dt$$

where $C_T(T)$ is the radioactivity concentration in a brain region, and $C_R(t)$ is the radioactivity concentration in the reference region. V and V' are the corresponding total distribution volumes (i.e., $V = K_1/k_2$, $V' = K_1'/k_2'$; k_2', the efflux rate constant from the reference tissue to plasma). b is the intercept term, which becomes constant for $T > t^*$. The k_2' value was estimated by the MRTM method (Ichise et al., 2002) and, to minimize the variability of k_2' estimation, a weighted mean k_2' value according to the VOI size over the raphe nucleus, thalamus, and striatum was calculated with the cerebellum as reference region, because postmortem studies indicated that the cerebellum cortex is almost devoid of 5-HTT (Kish et al., 2005; Varnas et al., 2004). BP_{ND} is then calculated from the two regression coefficients as,

$$BP_{ND} = -(\gamma_1/\gamma_2 + 1),$$

where $\gamma_1 = -V/(V'b)$ and $\gamma_2 = 1/b$, respectively.

Image data analysis

VOIs were placed on the standardized BP_{ND} images for the bilateral putamen; caudate nucleus; globus pallidus; thalamus and its subregions (pulvinar, mediodorsal, and anteriodorsal); hippocampal regions including the parahippocampus, uncus, and hippocampus; anterior and posterior cingulate; and the lateral temporal cortex, basal side as well as the convex side of the frontal cortex, parietal cortex, and occipital cortex (Fig. 1, Table I). The same VOI set was applied for both [^{11}C]WAY100635 and [^{11}C]DASB in all subjects.

Statistical analysis

Data are presented as mean ± SD. Pearson's correlation coefficient was calculated for the evaluation of correlation. Correction for multiple comparisons was not performed during the analysis because of the large number of correlations performed, and these results were considered exploratory. Laterality of the hemispheres was tested by performing a paired t-test for each region. SPSS package version 16 (SPSS, Chicago, IL) was used for statistical analysis.

RESULTS

For both radiotracers, parametric BP_{ND} images with anatomic standardization were obtained from 17 participants. The averaged images for all subjects are presented in Figures 2 and 3; mean and SD values of BP_{ND} are shown in Table II and Figure 4.

Distribution patterns of the 5-HTT and 5-HT_{1A} receptors in the human brain were measured with radioligands [^{11}C]DASB and [^{11}C]WAY100635, respectively, and they were observed to be quite different. The highest binding to 5-HTT was observed in the dorsal raphe nuclei, thalamus, and striatum. Moderate binding was observed in the insula, hippocampal area, and the anterior and posterior cingulate; very

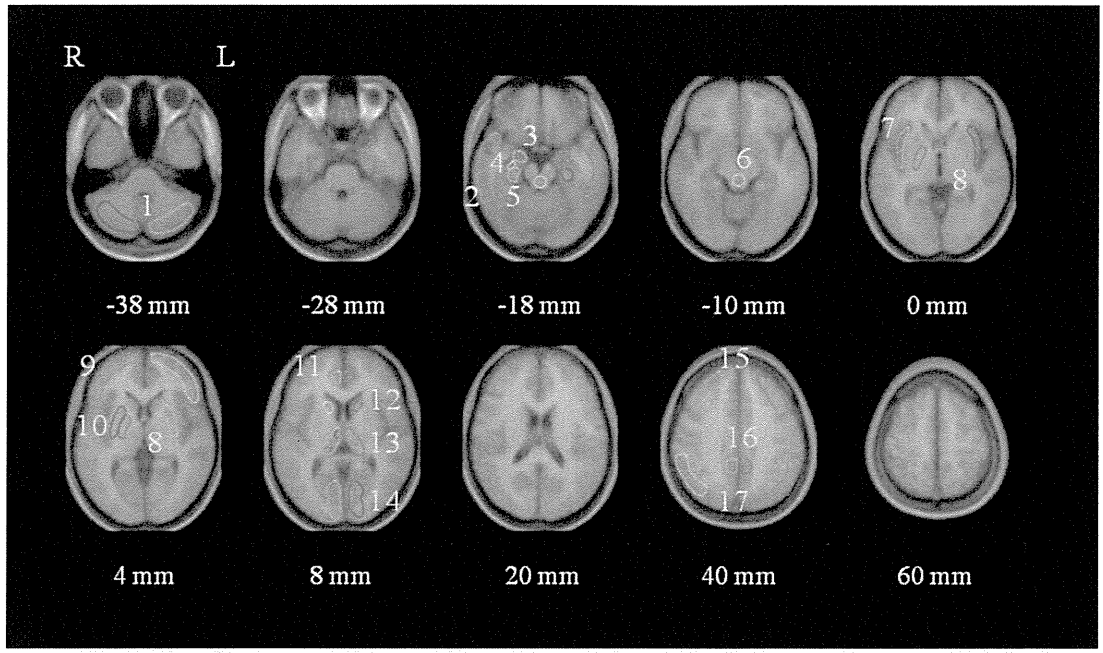

Fig. 1. VOIs drawn on the anatomically standardized MR images averaged for all subjects. Z = −38, −28, −18, −10, 0, 4, 8, 20, 40, 60 mm parallel to the anterior commissure and posterior commissure (AC-PC) line in the MNI template brain. L denotes left side of the brain; R denotes right side; 1, cerebellar cortex; 2, lateral temporal cortex; 3, uncus (amygdala); 4, hippocampus; 5, parahippocampal gyrus; 6, dorsal raphe nucleus; 7, insula; 8, globus pallidus; 9, base of frontal cortex; 10, putamen; 11, anterior cingulate; 12, head of caudate nucleus; 13, thalamus; 14, occipital cortex; 15, frontal convexity; 16, posterior cingulate; 17, parietal cortex.

TABLE I. Representative MNI coordinates and volumes in VOIs drawn on the MNI template image

	Right				Left				
Region	X	Y	Z	Volume (cm^3)	X	Y	Z	Volume (cm^3)	Total volume (cm^3)
Cerebellum	25	−70	−38	4.20	−31	−69	−38	4.30	8.50
Dorsal raphe nucleus	0	−31	−14						1.13
Striatum				1.69				1.99	3.68
Putamen	26	−1	4	1.34	−28	−2	4	1.54	2.88
Caudate head	14	14	8	0.35	−15	12	8	0.45	0.80
Globus Pallidus	20	−8	0	0.89	−18	−6	0	0.95	1.84
Thalamus	10	−23	8	1.67	−12	−22	8	1.60	3.27
Hippocampal complex				1.62				1.73	3.34
Uncus	21	−7	−18	0.70	−27	−24	−18	0.80	1.50
Hippocampus	29	−16	−18	0.19	−28	−13	−18	0.22	0.41
Parahippocampus	26	−24	−18	0.70	−27	−24	−18	0.80	1.50
Insula	38	4	−2	1.74	−38	3	−2	1.46	3.20
Anterior cingulate	5	43	8	0.53	−7	43	8	0.58	1.10
Posterior cingulate	6	−47	40	0.91	−9	−47	40	0.72	1.63
Base side of frontal cortex	34	45	4	4.58	−36	45	4	4.66	9.24
Frontal convexity	31	29	40	3.23	−35	24	40	3.25	6.51
Lateral temporal	53	−17	−18	5.58	−55	−17	−18	5.26	10.84
Occipital cuneus	13	−81	8	2.47	−9	−81	8	2.54	5.02
Parietal	49	−56	40	3.17	−51	−57	40	3.30	6.46

low binding was observed in the neocortical regions. In contrast, the highest binding to 5-HT_{1A} receptors was observed in the medial temporal regions including the hippocampus, uncus (amygdala), parahippocampus, and insula. Then, slightly lower binding was observed in the cingulate cortex and other cortical regions in descending order, with very low binding being seen in the basal ganglia and thalamus. As shown in Figure 4, when we divide brain regions into 5-HTT transporter rich regions and 5-HT_{1A} receptor rich regions, the relationships between mean values of BP_{ND} in 5-HTT and 5-HT_{1A} receptors were quite different. No linear correlation was found in 5-HTT transporter-rich regions between the mean values of BP_{ND} in 5-HTT and 5-HT_{1A} receptors, while a positive linear correlation, except the occipital cortex (r = 0.862, P = 0.006), was found between them in the 5-HT_{1A} receptor-rich regions.

There was no significant difference between the two sides of the brain with either of the radiotracers,

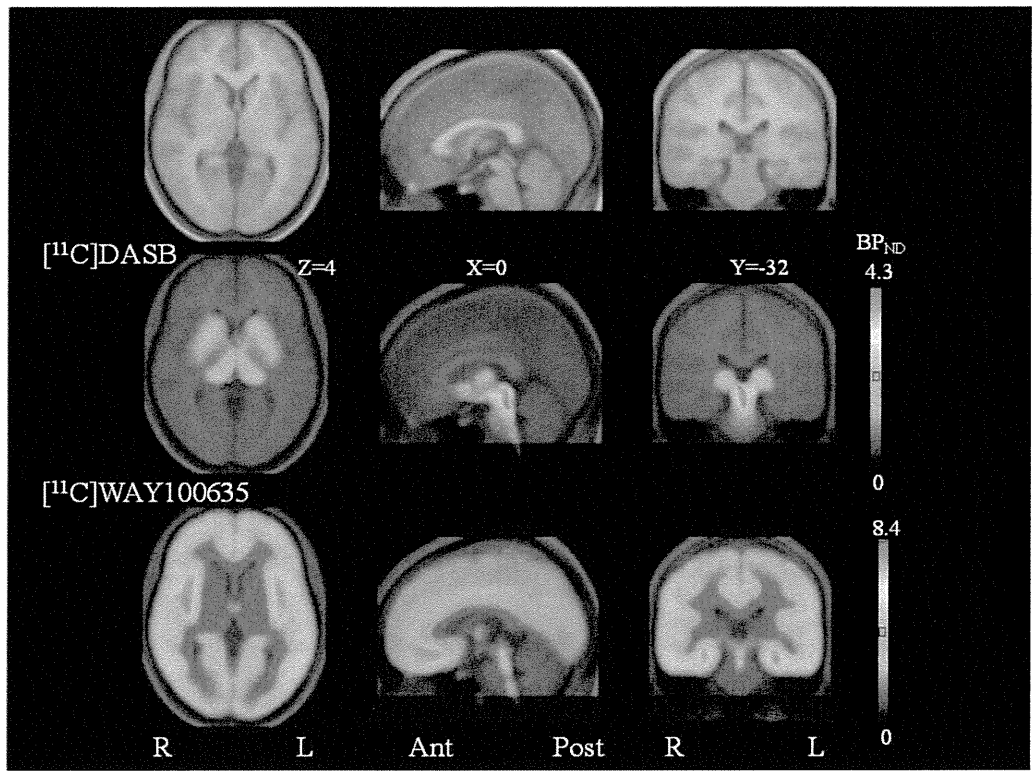

Fig. 2. Averaged images of MRI, [^{11}C]DASB image fused with MRI, and [^{11}C]WAY100635 image fused with MRI for all subjects. In left to right columns, transaxial, saggital, and coronal planes of the brain are displayed. X = 0 mm, Y = −32 mm, and Z = 4 mm indicate the coordinates of the three planes in the MNI template brain. R represents right; L, left. Ant indicates anterior; Post, posterior.

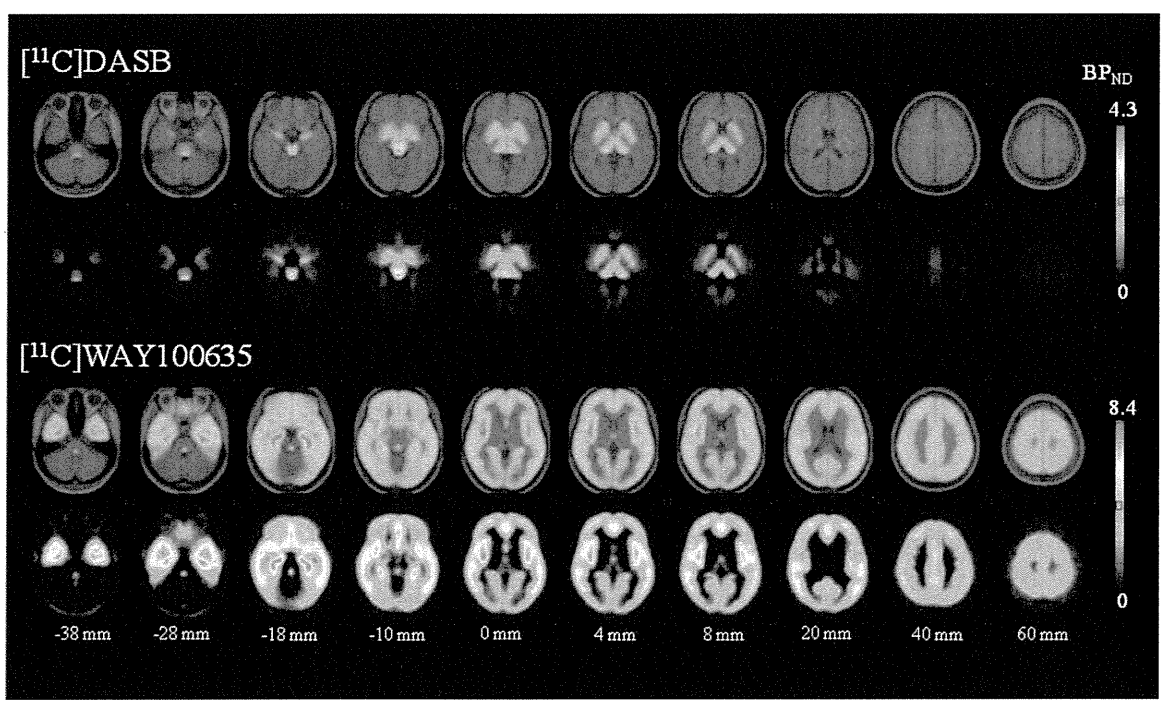

Fig. 3. Averaged BP_{ND} images with anatomical standardization of both radiotracers (axial planes). From the top row to the bottom: fused [^{11}C]WAY100635 and MRI, only [^{11}C]WAY100635, fused [^{11}C]DASB and MRI, only [^{11}C]DASB. In left to right columns: from ventral to dorsal planes of transverse images. L denotes left side of the brain; R denotes right side. Color bar indicates the value of BP_{ND}.

TABLE II. BPND values for each VOI

Region	[^{11}C]DASB			[^{11}C]WAY100635				
	Total	Right	Left	Total	Right	Left	*r*	*P*
Dorsal raphe nucleus	3.10 ± 0.97			2.17 ± 0.54			−0.191	0.464
Striatum	1.42 ± 0.28	1.40 ± 0.27	1.43 ± 0.30	1.42 ± 0.39	1.23 ± 0.38	1.58 ± 0.53	−0.333	0.192
Putamen	1.46 ± 0.29	1.45 ± 0.28	1.47 ± 0.30	1.72 ± 0.47	1.48 ± 0.48	1.94 ± 0.66	−0.368	0.146
Caudate head	1.25 ± 0.30	1.20 ± 0.28	1.29 ± 0.35	0.32 ± 0.23	0.29 ± 0.24	0.34 ± 0.25	0.208	0.423
Globus Pallidus	1.15 ± 0.36	1.14 ± 0.48	1.15 ± 0.31	0.35 ± 0.20	0.30 ± 0.22	0.40 ± 0.24	−0.446	0.073
Thalamus	1.88 ± 0.48	1.89 ± 0.53	1.87 ± 0.44	0.95 ± 0.27	1.03 ± 0.33	0.87 ± 0.26	−0.210	0.420
Anterior nucleus	1.93 ± 0.48	2.01 ± 0.57	1.84 ± 0.41	1.38 ± 0.41	1.37 ± 0.60	1.38 ± 0.34	−0.407	0.105
Dorsomedial nucleus	2.01 ± 0.51	2.08 ± 0.55	1.93 ± 0.50	1.23 ± 0.45	1.30 ± 0.55	1.16 ± 0.51	−0.328	0.199
Pulvinar	2.18 ± 0.73	2.03 ± 0.71	2.31 ± 0.79	0.89 ± 0.41	1.02 ± 0.43	0.77 ± 0.51	−0.079	0.762
Hippocampal complex	0.83 ± 0.18	0.83 ± 0.18	0.82 ± 0.19	6.30 ± 0.97	6.27 ± 1.03	6.33 ± 0.95	−0.306	0.232
Uncus	1.20 ± 0.27	1.18 ± 0.26	1.23 ± 0.29	5.78 ± 1.05	5.90 ± 1.10	5.66 ± 1.06	−0.268	0.297
Hippocampus	0.61 ± 0.18	0.58 ± 0.22	0.65 ± 0.17	7.01 ± 1.34	7.34 ± 1.55	6.71 ± 1.36	−0.226	0.383
Parahippocampus	0.52 ± 0.12	0.54 ± 0.13	0.51 ± 0.13	6.61 ± 1.03	6.36 ± 1.10	6.82 ± 1.11	−0.322	0.208
Insula	0.70 ± 0.17	0.75 ± 0.19	0.65 ± 0.15	6.65 ± 1.13	6.64 ± 1.14	6.67 ± 1.20	*−0.506	0.038
Anterior cingulate	0.45 ± 0.09	0.42 ± 0.11	0.47 ± 0.10	5.39 ± 0.83	5.46 ± 0.93	5.33 ± 0.90	*−0.539	0.026
Posterior cingulate	0.35 ± 0.07	0.37 ± 0.07	0.33 ± 0.10	4.76 ± 0.69	4.91 ± 0.73	4.57 ± 0.81	*−0.484	0.049
Base side of frontal cortex	0.21 ± 0.07	0.22 ± 0.08	0.20 ± 0.06	4.45 ± 0.76	4.54 ± 0.80	4.36 ± 0.75	*−0.539	0.026
Frontal convexity	0.20 ± 0.06	0.20 ± 0.06	0.19 ± 0.06	4.55 ± 0.82	4.53 ± 0.78	4.56 ± 0.87	−0.464	0.061
Lateral temporal	0.25 ± 0.05	0.26 ± 0.06	0.23 ± 0.05	5.73 ± 0.86	5.70 ± 0.86	5.76 ± 0.87	*−0.603	0.010
Occipital cuneus	0.39 ± 0.10	0.38 ± 0.11	0.40 ± 0.11	2.59 ± 0.51	2.55 ± 0.56	2.62 ± 0.51	−0.433	0.083
Parietal	0.12 ± 0.04	0.13 ± 0.04	0.12 ± 0.04	4.54 ± 0.71	4.61 ± 0.73	4.46 ± 0.74	*−0.718	0.001

r indicates Pearson's correlation coefficients between total BPND of [^{11}C]DASB and that of [^{11}C]WAY100635 for each VOI.
*Indicates $P < 0.05$.

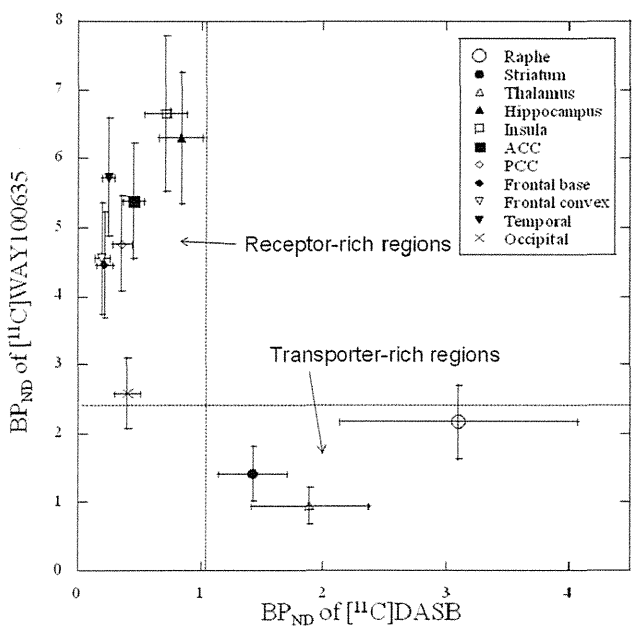

Fig. 4. Relationships between mean BP_{ND} values of [^{11}C]DASB and those of [^{11}C]WAY100635. The error bars indicate standard deviation.

indicating no apparent laterality in the distribution of 5-HTT and 5-HT_{1A} (paired *t*-test, data not shown). Moreover, no significant correlation between age and the binding of 5-HTT and 5-HT_{1A} was found in any of the brain regions within the age range (20–40 yr) of our sample (Pearson's correlation coefficient, $P > 0.05$, data not shown). In addition, with regard to the intraindividual relationship between the binding of both [^{11}C]DASB and [^{11}C]WAY100635 in the same region of the brain, significant negative correlations were observed in the anterior and posterior cingulate, insula, basal side of the frontal cortex, lateral temporal cortex, and parietal cortex (Table II and Fig. 5), whereas no significant positive correlation was observed.

DISCUSSION

We constructed a database of 5-HTT and 5-HT_{1A} serotonergic function by using parametric images generated by the anatomic standardization of the brains of 17 healthy young men. Anatomical standardization enables visualization of the entire neuroanatomy along the same coordinates with the help of multiple radiotracers that permit inter- and intrasubject comparisons. In the current study, the distributions of the two serotonergic markers differed. In addition, an exploratory study revealed significant inverse linear correlations between BP_{ND} of presynaptic 5-HTT and that of postsynaptic 5-HT_{1A} receptor binding in certain areas of the brain, such as the frontal, temporal, and parietal cortices; insula; and anterior and posterior cingulate.

Overall, the distribution patterns of 5-HTT and 5-HT_{1A} binding in the human brain were in accordance with those observed in previous human PET and postmortem studies (Brust et al., 2006; Drevets et al., 2007; Hall et al., 1997; Hoyer et al., 1986; Ito et al., 1999; Kish et al., 2005; Laruelle et al., 1988; Pazos et al., 1987; Rabiner et al., 2002; Savitz et al., 2009; Stockmeier, 2003; Varnas et al., 2004).

Localization of 5-HTT and 5-HT_{1A} in respective regions of the brain

In general, distributions in 5-HTT and 5-HT_{1A} receptors are quite different, and can be categorized into two groups, 5-HTT-rich regions and 5-HT_{1A} receptor-rich regions (Fig. 4). In 5-HT_{1A} receptor-rich regions such as the cerebral cortex and limbic

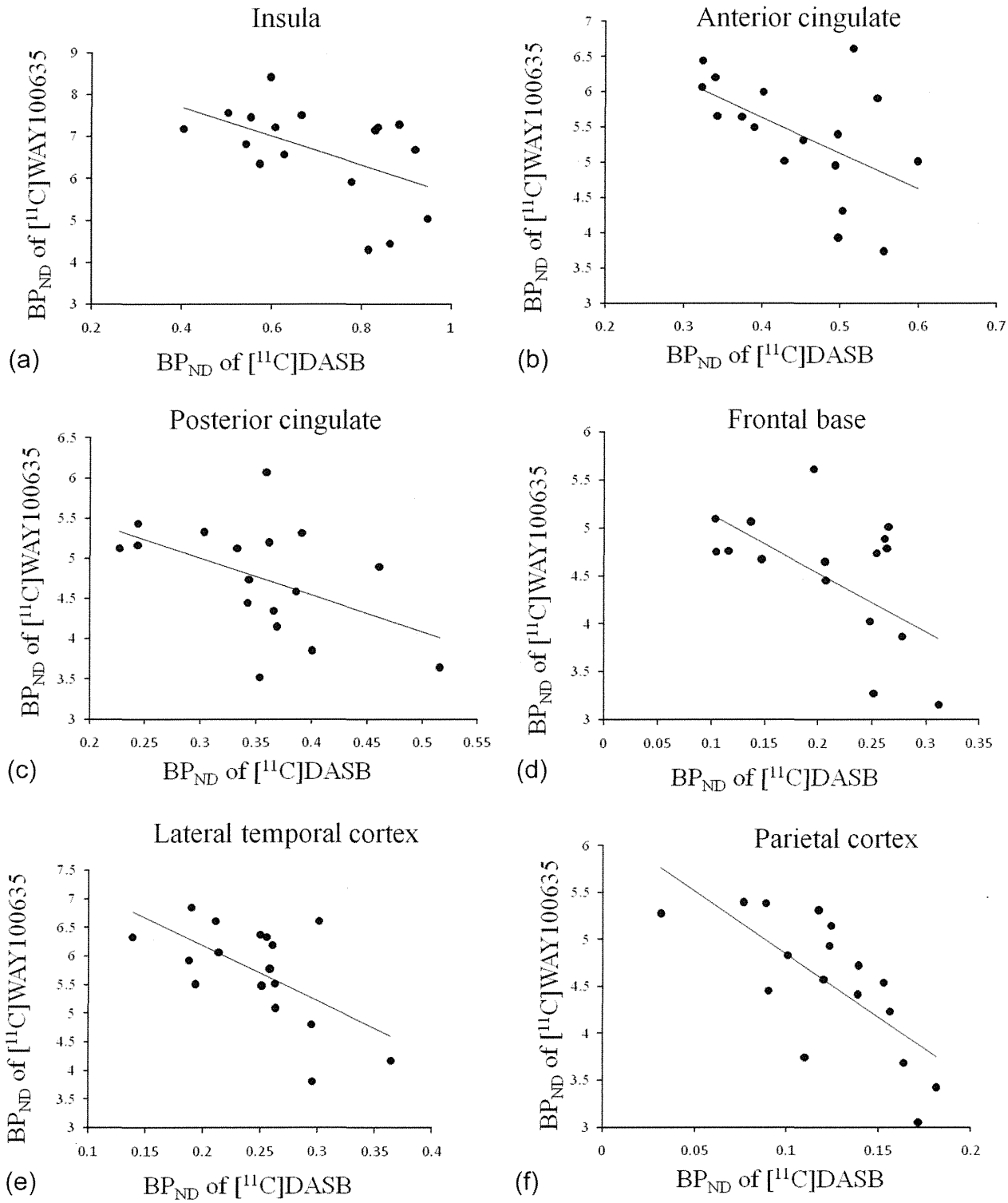

Fig. 5. Areas showing significant correlations of BP_{ND} values between [^{11}C]DASB and [^{11}C]WAY100635 in intrasubject comparisons. (a) insula, (b) anterior cingulate, (c) posterior cingulate, (d) base side of frontal cortex, (e) lateral temporal cortex, (f) parietal cortex.

regions, they tend to positively correlate with each other except the occipital cortex. This finding could reflect innervation of serotonergic fibers in those regions.

5-HTT-rich region

Brain stem. High binding to 5-HTT was observed in large areas of the midbrain, and it continuously

extended to the thalamus; this finding indicated rich distribution in these regions. In contrast, moderate binding to 5-HT_{1A} receptors was observed only in the dorsal and medial raphe, with this distribution indicating that 5-HT_{1A} receptor exists only in these regions of the midbrain (the sagittal section, middle column in the bottom row in Figure 2; the transverse sections, the first to fourth columns in the second row from the bottom; further, refer to the volume of interest 6 in Figure 1, which represents the raphe nuclei). These distribution patterns of 5-HTT and 5-HT_{1A} were consistent with those observed in previous human postmortem autoradiography studies (Hall et al., 1997; Varnas et al., 2004). In the present study, however, 5-HT_{1A} binding was not very high as compared with that in other areas (Table II). For example, the mean BP_{ND} value in the dorsal raphe was approximately one-third of that in the hippocampus, which exhibited the highest value of all regions examined. Further, in a detailed human autoradiography study with [^{3}H]WAY100635, binding to the dorsal raphe was highest (140 pmol/g tissue), followed by the hippocampus (123 pmol/g tissue). However, this discrepancy may be a result of the limited spatial resolution of the PET scanner, resulting in excessive spillover from the raphe and other small structures.

Subcortical regions. In the striatum (putamen and caudate) and globus pallidus, relatively high levels of binding to 5-HTT were observed. In contrast, 5-HT_{1A} receptor binding was very low or absent in the caudate nucleus and globus pallidus, while a low level of binding was found in the putamen. However, postmortem autoradiography studies showed very low levels of binding in the putamen, similar to those in the caudate and globus pallidus (Hall et al., 1997; Varnas et al., 2004); the high BP_{ND} values in the putamen may be attributed to spillover from the insula, which exhibits a very high level of 5-HT_{1A} binding.

The level of 5-HTT binding in the thalamus was the second highest among all brain regions, after the dorsal raphe nucleus; further, there was no marked difference in 5-HTT distribution among the subregions of the thalamus. These findings were similar to those of a previous human postmortem study (Varnas et al., 2004). On the other hand, the level of binding to the 5-HT_{1A} receptor was very low in the thalamus, although a little binding was observed in its medial parts regions (Table II and Figs. 2–4); this finding was similar to those of previous autoradiography studies showing much less or no binding in these regions (Hall et al., 1997; Varnas et al., 2004).

5-HT_{1A} receptor-rich region

Cerebral neocortex. Relatively high binding to 5-HT_{1A} and low binding to 5-HTT were observed in the neocortical regions. The 5-HT_{1A} receptor was widely distributed in the cerebral cortex but sparsely in the occipital cortex. The distribution of 5-HTT was very low in the neocortical regions as compared with other brain regions, but was found to be homogeneous among the cortical regions (Figs. 2–4, Table II). These findings were consistent with those of previous postmortem autoradiography studies (Hall et al., 1997; Laruelle et al., 1988; Varnas et al., 2004).

Limbic regions. In the hippocampal regions that include the parahippocampus, hippocampus, and uncus (amygdala), highest binding to 5-HT_{1A} and moderate binding to 5-HTT were observed (Figs. 2–4, Table II). Postmortem autoradiography studies in humans revealed that the highest binding to 5-HT_{1A} was observed particularly over the CA1 field in the hippocampus (Hall et al., 1997; Varnas et al., 2004). In contrast, binding to 5-HTT was higher in the uncus as compared to other hippocampal regions, a finding in agreement with a previous postmortem study (Varnas et al., 2004).

Within the cingulate cortex, both 5-HTT and 5-HT_{1A} binding can be described in descending order as follows: ventral (subcallosal) cingulate > anterior cingulate > posterior cingulate (Table II and Figs 2 and 3). In particular, the ventral cingulate is thought to be involved in the regulation of emotions and has been repeatedly reported to be associated with depression (Drevets et al., 2008; Seminowicz et al., 2004).

Very high 5-HT_{1A} binding and intermediate 5-HTT binding were observed in the insula. These distributions are in accordance with those found in previous human postmortem autoradiography studies (Varnas et al., 2004), although BP_{ND} values in the insula can be affected by spillover from the striatum, which exhibits high levels of 5-HTT binding.

Our findings together suggest that the limbic regions, including the hippocampal area, cingulate cortex, and insula, are relatively rich in serotonergic innervation. Thus, serotonergic transmission in these regions might play a pivotal role in modulating emotion and cognition.

Intraindividual relationship between the binding of both [^{11}C]DASB and [^{11}C]WAY100635 in the same region of the brain

With respect to the intraindividual relationship between regional 5-HTT and 5-HT_{1A} distribution, we found significant negative linear correlations between the binding of [^{11}C]DASB and [^{11}C]WAY100635 in the insula; anterior and posterior cingulate; and lateral temporal, frontal base, and parietal cortices. This result suggests that serotonergic transmission might be modulated by a cooperative relationship between 5-HTT and 5-HT_{1A}.

There have been only a few reports on pre- and postsynaptic serotonergic functions in individuals. In a study of 12 men, Lundberg et al. (2007) showed a positive linear correlation between 5-HTT and 5-HT_{1A} binding in the raphe nuclei and hippocampal complex using [^{11}C]MADAM and [^{11}C]WAY100635, respectively; however, a positive linear correlation was not observed in the frontal cortex. Another study that examined gender differences in binding using [^{11}C]MADAM and [^{11}C]WAY100635 also reported an interrelationship between 5-HTT and 5-HT_{1A} receptors (Jovanovic et al., 2008). They found a significant positive correlation between BP_{ND} of 5-HTT and 5-HT_{1A} receptors in the hippocampus of eight women, whereas no significant correlation was observed in seven men. The discrepancy between their results and ours could be attributed to the use of different 5-HTT radiotracers, sample size, and subjects' background. In particular, the age range of subjects in the study by Lundberg et al. was wider than ours, and different degrees of atrophy can cause positive correlation in BP_{ND} between 5-HTT and 5-HT_{1A} receptor. This is because older subjects are likely to have more brain atrophy, because of which both BP_{ND} values are lower than those of young subjects. Our results suggest that subjects exhibiting higher 5-HTT binding are likely to have less 5-HT_{1A} receptor binding and vice versa. One possible interpretation of this intersubject difference is that individuals with higher 5-HT synthesis and release show a decrease in the 5-HT_{1A} receptor function to dampen the transmission at the postsynaptic site and an increase in 5-HTT function in order to reuptake more 5-HT at the presynaptic site, whereas individuals with lower 5-HT synthesis and release show an increase in the 5-HT_{1A} receptor function and a decrease in 5-HTT function to reuptake less 5-HT; that is, pre- and postsynaptic 5-HT functions are modulated cooperatively to compensate the overall 5-HT transmission. However, these studies were done under resting condition, and therefore challenge study designs using drugs or stress may help to better understand the relationship between pre- and postsynaptic functions.

Limitation

There are several limitations to the current study. First, the two PET studies were not always performed on the same day. Good reproducibility for both ligands (Kim et al., 2006; Rabiner et al., 2002), however, has been demonstrated, and it has been shown that the endogenous 5-HT level has no direct effect on binding (Rabiner et al., 2002; Talbot et al., 2005); hence, it is unlikely that the endogenous level affected the results. Second, the sample size was small, especially for a correlation study between pre- and postsynaptic functions, and our study should necessarily be regarded as a preliminary one. Third, we focused only on 5-HTT and 5-HT_{1A} receptors because they reportedly play pivotal roles in serotonergic functions. However, there are more than 10 receptor systems in the brain that affect serotonergic transmission. In addition, monoamine oxidase as well as 5-HTT are known to control the 5-HT concentration in the synapse (Nestler et al., 2008). Finally, the current study includes only young men, and we should expand it to women and individuals of a wider range of ages. Such a database will be helpful even for clinical studies on depression and anxiety disorders, since these disorders are known to show different prevalence and clinical features depending on gender and age (Fernandez et al., 1995; Gorman, 2006; Pigott, 1999). The physiological differences in the 5-HT system based on gender and age might explain the characteristics of depression and anxiety disorders.

In summary, we constructed a normal database to elucidate regional distributions of 5-HT_{1A} and 5-HTT binding. The neuroanatomy of the 5-HT_{1A} and 5-HTT serotonergic systems was discussed mostly by comparing our findings with those of previous postmortem studies. Furthermore, we explored the linear negative correlation between pre- and postsynaptic functions in certain parts of the brain. The results obtained indicate the involvement of a cooperative or complementary process in serotonergic transmission. Further studies are required to elucidate the modulation of 5-HT transmission in neuropsychiatric disorders and to clarify the various serotonergic systems involving pre- and postsynaptic functions in different regions of the brain.

ACKNOWLEDGMENTS

The authors thank Mr. Katuyuki Tanimoto, Mr. Takahiro Shiraishi, and Mr. Akira Ando for their assistance in performing PET examinations at the National Institute of Radiological Sciences. The authors are also grateful to Ms. Yoshiko Fukushima for the help as a clinical research coordinator.

REFERENCES

Brust P, Hesse S, Muller U, Szabo Z. 2006. Neuroimaging of the serotonin transporter. Curr Psychiatry Rev 2:111–149.
Cooper JR, Bloom FE, Roth RH. 2002. The biochemical basis of neuropharmacology, 8th ed. New York, USA: Oxford University Press.
Diksic M, Young SN. 2001. Study of the brain serotonergic system with labeled alpha-methyl-L-tryptophan. J Neurochem 78:1185–1200.
Drevets WC, Savitz J, Trimble M. 2008. The subgenual anterior cingulate cortex in mood disorders. CNS Spectr 13:663–681.
Drevets WC, Thase ME, Moses-Kolko EL, Price J, Frank E, Kupfer DJ, Mathis C. 2007. Serotonin-1A receptor imaging in recurrent depression: replication and literature review. Nucl Med Biol 34:865–877.
Fernandez F, Levy JK, Lachar BL, Small GW. 1995. The management of depression and anxiety in the elderly. J Clin Psychiatry 56(Suppl 2):20–29.
Gorman JM. 2006. Gender differences in depression and response to psychotropic medication. Gend Med 3:93–109.

Gunn RN, Lammertsma AA, Hume SP, Cunningham VJ. 1997. Parametric imaging of ligand-receptor binding in PET using a simplified reference region model. Neuroimage 6:279–287.

Gunn RN, Sargent PA, Bench CJ, Rabiner EA, Osman S, Pike VW, Hume SP, Grasby PM, Lammertsma AA. 1998. Tracer kinetic modeling of the 5-HT1A receptor ligand [carbonyl-^{11}C]WAY-100635 for PET. Neuroimage 8:426–440.

Hall H, Lundkvist C, Halldin C, Farde L, Pike VW, McCarron JA, Fletcher A, Cliffe IA, Barf T, Wikstrom H, Sedvall G. 1997. Autoradiographic localization of 5-HT$_{1A}$ receptors in the post-mortem human brain using [^{3}H]WAY-100635 and [^{11}C]way-100635. Brain Res 745:96–108.

Hoyer D, Hannon JP, Martin GR. 2002. Molecular, pharmacological and functional diversity of 5-HT receptors. Pharmacol Biochem Behav 71:533–554.

Hoyer D, Pazos A, Probst A, Palacios JM. 1986. Serotonin receptors in the human brain. I. Characterization and autoradiographic localization of 5-HT$_{1A}$ recognition sites. Apparent absence of 5-HT$_{1B}$ recognition sites. Brain Res 376:85–96.

Ichise M, Liow JS, Lu JQ, Takano A, Model K, Toyama H, Suhara T, Suzuki K, Innis RB, Carson RE. 2003. Linearized reference tissue parametric imaging methods: application to [^{11}C]DASB positron emission tomography studies of the serotonin transporter in human brain. J Cereb Blood Flow Metab 23:1096–1112.

Ichise M, Toyama H, Innis RB, Carson RE. 2002. Strategies to improve neuroreceptor parameter estimation by linear regression analysis. J Cereb Blood Flow Metab 22:1271–1281.

Innis RB, Cunningham VJ, Delforge J, Fujita M, Gjedde A, Gunn RN, Holden J, Houle S, Huang SC, Ichise M, Iida H, Ito H, Kimura Y, Koeppe RA, Knudsen GM, Knuuti J, Lammertsma AA, Laruelle M, Logan J, Maguire RP, Mintun MA, Morris ED, Parsey R, Price JC, Slifstein M, Sossi V, Suhara T, Votaw JR, Wong DF, Carson RE. 2007. Consensus nomenclature for in vivo imaging of reversibly binding radioligands. J Cereb Blood Flow Metab 27:1533–1539.

Ito H, Halldin C, Farde L. 1999. Localization of 5-HT$_{1A}$ receptors in the living human brain using [carbonyl-^{11}C]WAY-100635: PET with anatomic standardization technique. J Nucl Med 40:102–109.

Ito H, Takahashi H, Arakawa R, Takano H, Suhara T. 2008. Normal database of dopaminergic neurotransmission system in human brain measured by positron emission tomography. Neuroimage 39:555–565.

Jovanovic H, Lundberg J, Karlsson P, Cerin A, Saijo T, Varrone A, Halldin C, Nordstrrom A-L. 2008. Sex differences in the serotonin 1A receptor and serotonin transporter binding in the human brain measured by PET. Neuroimage 39:1408–1419.

Kim JS, Ichise M, Sangare J, Innis RB. 2006. PET imaging of serotonin transporters with [^{11}C]DASB: test-retest reproducibility using a multilinear reference tissue parametric imaging method. J Nucl Med 47:208–214.

Kish SJ, Furukawa Y, Chang LJ, Tong J, Ginovart N, Wilson A, Houle S, Meyer JH. 2005. Regional distribution of serotonin transporter protein in postmortem human brain: is the cerebellum a SERT-free brain region? Nucl Med Biol 32:123–128.

Kitson SL. 2007. 5-hydroxytryptamine (5-HT) receptor ligands. Curr Pharm Des 13:2621–2637.

Kumar JSD, Mann JJ. 2007. PET tracers for 5-HT(1A) receptors and uses thereof. Drug Discov Today 12:748–756.

Lammertsma AA, Hume SP. 1996. Simplified reference tissue model for PET receptor studies. Neuroimage 4:153–158.

Laruelle M, Vanisberg MA, Maloteaux JM. 1988. Regional and subcellular localization in human brain of [^{3}H]paroxetine binding, a marker of serotonin uptake sites. Biol Psychiatry 24:299–309.

Lundberg J, Borg J, Halldin C, Farde L. 2007. A PET study on regional coexpression of 5-HT$_{1A}$ receptors and 5-HTT in the human brain. Psychopharmacology 195:425–433.

Lundquist P, Blomquist G, Hartvig P, Hagberg GE, Torstenson R, Hammarlund-Udenaes M, Langstrom B. 2006. Validation studies on the 5-hydroxy-L-[beta-^{11}C]-tryptophan/PET method for probing the decarboxylase step in serotonin synthesis. Synapse 59:521–531.

Marner L, Gillings N, Comley RA, Baare WF, Rabiner EA, Wilson AA, Houle S, Hasselbalch SG, Svarer C, Gunn RN, Laruelle M, Knudsen GM. 2009. Kinetic modeling of ^{11}C-SB207145 binding to 5-HT$_{4}$ receptors in the human brain in vivo. J Nucl Med 50:900–908.

Meyer JH. 2007. Imaging the serotonin transporter during major depressive disorder and antidepressant treatment. J Psychiatry Neurosci 32:86–102.

Moresco RM, Matarrese M, Fazio F. 2006. PET and SPET molecular imaging: Focus on serotonin system. Curr Top Med Chem 6:2027–2034.

Nestler E, Hyman S, Malenka R. 2008. Molecular neuropharmacology: A foundation for clinical neuroscience, 2nd ed. New York, USA: McGraw-Hill Professional.

Pazos A, Probst A, Palacios JM. 1987. Serotonin receptors in the human brain. III. Autoradiographic mapping of serotonin-1 receptors. Neuroscience 21:97–122.

Pigott TA. 1999. Gender differences in the epidemiology and treatment of anxiety disorders. J Clin Psychiatry 60(Suppl 18):4–15.

Rabiner EA, Messa C, Sargent PA, Husted-Kjaer K, Montgomery A, Lawrence AD, Bench CJ, Gunn RN, Cowen P, Grasby PM. 2002. A database of [^{11}C]WAY-100635 binding to 5-HT$_{1A}$ receptors in normal male volunteers: Normative data and relationship to methodological, demographic, physiological, and behavioral variables. Neuroimage 15:620–632.

Savitz J, Lucki I, Drevets WC. 2009. 5-HT$_{1A}$ receptor function in major depressive disorder. Prog Neurobiol 88:17–31.

Seminowicz DA, Mayberg HS, McIntosh AR, Goldapple K, Kennedy S, Segal Z, Rafi-Tari S. 2004. Limbic-frontal circuitry in major depression: A path modeling metanalysis. Neuroimage 22:409–418.

Stockmeier CA. 2003. Involvement of serotonin in depression: Evidence from postmortem and imaging studies of serotonin receptors and the serotonin transporter. J Psychiatr Res 37:357–373.

Suhara T, Sudo Y, Yoshida K, Okubo Y, Fukuda H, Obata T, Yoshikawa K, Suzuki K, Sasaki Y. 1998. Lung as reservoir for antidepressants in pharmacokinetic drug interactions. Lancet 351:332–335.

Talbot PS, Frankle WG, Hwang DR, Huang Y, Suckow RF, Slifstein M, Abi-Dargham A, Laruelle M. 2005. Effects of reduced endogenous 5-HT on the in vivo binding of the serotonin transporter radioligand ^{11}C-DASB in healthy humans. Synapse 55:164–175.

Varnas K, Halldin C, Hall H. 2004. Autoradiographic distribution of serotonin transporters and receptor subtypes in human brain. Hum Brain Mapp 22:246–260.